ISME

Vibration Attenuation Timoshenko Beam Based on Optimal Placement Sensors/ Actuators PZT Patches with LQR-MOPSO

M. Hasanlu*
MSc. Graduate

M. Siavashi†
Professor

A. Bagheri‡
Professor

The main objective of this study is to reduce optimal vibration suppression of Timoshenko beam under non-periodic step and impulse inputs. Cantilever beam was modeled by Timoshenko theory and finite element numerical method. Then, in order to control structure vibration, piezoelectric patches were used due to simultaneous dual behavior, i.e. switching mechanical behavior to electrical behavior (sensor) and electrical behavior to mechanical behavior (actuator). Piezoelectric patches are used in two different arrays with equal dimensions and different elements for establishing feedback control. In the following, by using linear quadratic regulator controller (LQR), structure vibrations became attenuated. Weighting coefficients of R and Q matrices and piezoelectric patch location have been searched by multi-objective particle swarm optimization algorithm (MOPSO). Finally, the structure underwent standard inputs of impulse and step and the results are analyzed and compared.

Keywords : Vibration Attenuation, Timoshenko Beam, Optimal placement, PZT Patches, LQR-MOPSO

1 Introduction

Today, engineering structures have wide application in military equipment, industrial equipment, machines, robots, etc. How to make the engineering structures away from many damages, repairs, and other costs and how to control them in a way that their life reduction would be prevented are challenging problems for researches in recent decades. They are trying to find an appropriate control approach by analyzing dynamic behavior to control unwanted vibrations from beams. Different control approaches have been suggested by designers for vibration control of an engineering structure. However, the extent to which it could meet the industry requirements is a problem investigated by engineers through optimization science and its combination with control rules.

*Corresponding Author, MSc. Graduate Student, Faculty of Mechanical Engineering, University of Guilan, mhasanlu@webmail.guilan.ac.ir
† Professor, Faculty of Mechanical Engineering, University of Guilan, bagheri@guilan.ac.ir
‡ Professor, Faculty of Mechanical Engineering, University of Guilan, fnajafi@guilan.ac.ir

Many researchers presented different control criteria and models in optimal positioning of piezoelectric elements on engineering structures such as beam and they attempted to attenuate the structures against fluctuations. S.T. Quek et al. investigated the vibration suppression of multilayer composite plate as cantilever and four sides clamped and find the best place for locating the piezoelectric sensor and actuator. By using finite element, they completed a numerical modeling. By using two perspectives, one of them based on controllability of mode and the other based on controllability of intelligent system, they extracted the objective function. Finally, they used Direct Pattern Search method (DPS) to optimize these objective functions and presented their results [1]. W. Liu et al. optimized the location of the piezoelectric sensor and actuator by using H_2 controller and genetic algorithm. During the simulation of their model, they used H_2 soft performance index as a good performance index in order to control the vibration of a plate with two simply supports [2]. H.Y. Guo et al. conducted the optimal placement of piezoelectric sensor and actuator on a truss structure by using genetic algorithm. Their objective was to keep this structure safe against external stimuli; it means that their objective function was considered according to the fault detection in system. But they implemented

Several reforms and suggestions in genetic algorithm: firstly, they used Penalty Function Method. Second, they used Force Mutation Method to increase the convergence rate of algorithm to the most efficient possible locations for placement of piezoelectric [3]. T.L. Da Rocha et al. conducted the optimal placement of piezoelectric on a cantilever plate as sensor and actuator by using H00 soft concept. Modeling of structure was done by using finite element with ANSYS and MATLAB software by using H_∞ and Linear Matrix Inequalities (LMI) method, they calculated the location of sensor and actuator on structure which finally resulted in vibration suppression due to the optimal placement of piezoelectric [4]. S.L dos. Santos e Lucato et al. generally conducted the optimal placement of piezoelectric sensor and actuator on a truss structure called Kagome Truss and their optimization algorithm included annealing and genetic algorithms and had good results from this research [5].

M.Brasseur et al. conducted the optimal placement of piezoelectric on an acoustic structure called Wooden Shutter Box by using controllability gramian index. The modeling method of this structure included finite element. The objective of this experimental and theoretical research was reaching desirable coordinates for the placement of piezoelectric in order to absorb sound in the room's environment [6]. H.H.Ning in an article investigated and optimized the place and number of piezoelectric on a cantilever plate as sensor and actuator to control the undesirable vibrations in the structure. In order to search the working environment of cantilever plate, genetic algorithm was used to find the best location of piezoelectric sensor and actuator [7]. A.S.D. Oliveira et al. conducted the optimal placement of piezoelectric sensor and actuator patches to form an intelligent structure on a simply support beam by using classic optimization. They extracted the critical coordinates by deriving figure function and put it equal to zero and by the placement of piezoelectric on these specific coordinates, they controlled its vibration. For controlling the system, they used Singular Value Decomposition (SVD) method as the objective function [8]. S.Y. Wang et al. optimized the location of piezoelectric sensor and actuator on a cantilever plate.

In this research, they considered piezoelectric sensor and actuator as isotropic and anisotropic so that can damp torsional vibrations of a composite plate. Modeling of composite plate was used through finite element which was based on the first order shear method and genetic algorithm was used to conduct the optimization process [9]. J. Lottin et al. in a descriptive article studied the optimal placement piezoelectric sensor and actuator on a structure. During four sections, they described placement methods, type of actuator and sensor in terms of efficiency and performance, type of structure, methods of assembling piezoelectric on a structure, methods of controlling system and place optimization criteria [10].

C. Swann et al. by exclusive placement of piezoelectric sensor on a composite plate with boundary conditions of cantilever and four sides clamped, tried to find delamination phenomenon in structure due to vibration. Modeling structure was done by using finite element based on Refined Layer-wise Theory (RLWT).

For conducting the optimization process for the place and number of sensors, genetic algorithm and Monte-Carlo Method was used to produce the initial population. Their objective was a troubleshooting method due to the optimal location of piezoelectric sensor for detection of composite delamination because of receiving voltage signals and comparing it to the non-delamination situation [11]. A.Belloli et al. analyzed the placement of piezoelectric ceramic pieces to neutralize the vibrations in rear wings of a race car. Optimization was done by using CATIA V5, ANSYS 9.0 and DynOPS software and it was completely designed and analyzed. The objective of optimization in this research was finding the best size, place and direction for the placement of piezoelectric and interesting results were extracted [12].

Zhi-Cheng. Qiu in their article studied cantilever plate model analytically and by using controllability degree and observability index of system, they optimized the placement of piezoelectric for vibration depression of structure. In this article, they tried to control the vibration of plate by combining two control methods including PPF and PDC (Proportional

Derivative Control). The type of studied vibration was torsional and flexural vibration. By making the torsional and flexural coupling relations independent through Bandwidth Butterworth Filter (BBF) method, they analyzed the vibration of system and applied controlling rules on them [13]. T. Roy et al. conducted a research on the optimal placement of piezoelectric patches by using genetic optimization algorithm and quadratic optimal control or LQR method. Their studied structures included Spherical composite panel, a cantilever composite beam and a composite plate. One of the innovations in this study was using multilayered piezoelectric composite pieces as sensor and actuator. By incorporating LRQ method and algorithm, it can be said that in LQR method, 3 coefficients in R and Q fixed matrixes are defined and by using genetic algorithm, the most optimized answer for these three coefficients is obtained. Finally, by the placement of these coefficients in energy relationship, the best places for actuator and sensor can be suggested [14].

M.R. Safizade et al. studied the optimal place for a plate with all edges clumped by using controllability gramian performance index and genetic algorithm. Structural equations of plate were extracted analytically and were incorporated with analytical equations of piezoelectric actuator and the equation of an intelligent structure was obtained. Then by using a controlling method, the optimal placement of their system was conducted. In this method, the main responsibility is system's controllability and expressing an optimum control input so that by applying forces on this optimal place of structure, system, can be damped [15].

J. Yang et al. in two researchers studied the optimal placement of piezoelectric sensor and actuator on a plate. Their theory was that in order to increase the controlling performance of system or in other words controlling the system by piezoelectric results in vibration suppression, piezoelectric actuator should affect a specific direction on plate. Now there are coordinates on the plate that show their potential effect by the placement of piezoelectric actuator and system is controlled more efficiently. They used two types of Simulated Annealing for the TSP (SATSP) algorithm and another algorithm called Hopfield-Tank for the TSP (HTTSP) to optimize the place of plate. The results of SATSP optimization algorithm were better than HTTSP. In this article, by using SATSP algorithm alongside Genetic Algorithm for TSP (GATSP) algorithm, better results from GATSP were provided compared to SATTSP [16-17]. V. Gupta et al. in a practical and helpful research used 6 objective functions for optimizing the placement of piezoelectric as sensor and actuator on the structure of beam and plate. These functions include [18]:

1) The maximization of force or torque released from piezoelectric actuator
2) The maximization of deflection in a structure
3) The minimization of controlling effect or the maximization of wasted energy
4) The maximization of controllability degree
5) The maximization of observability degree
6) The minimization of spillover phenomenon

M. Trajkov et al. analyzed the placement based on controllability and observability criteria. The optimization was conducted based on H2 and H00 soft and controllability and observability gramian function which is dependent on vibrational modes. The structure model was designed using finite element and after the reduction of order process, optimization operations were done on the reduced model and the optimal place was suggested for the plate and cantilever beam [19]. F. Bachman et al. conducted a research on optimal placement of two piezoelectric pieces on a turbo machinery blade which is a carbon / epoxy composite and by using the criterion of increasing potential energy for piezoelectric and structure and increasing electromechanical coupling damping coefficient, they tried to increase the energy saved in piezoelectric in the best place of a composite blade [20].

J. Zhang et al. analyzed the vibration suppression of a cantilever beam by finding the best place in that beam for the placement of piezoelectric actuator and sensor in order to from an intelligent system for automatically controlling of the vibration and reaching a logical stability. For system's steering, they used Linear Quadratic Gauss (LQC) controller as an optimal controller method and analyzed 4 vibration modes of beam [21]. A. Molter et al. studied the optimal placement of piezoelectric on a flexible Manipulator as a cantilever beam with its mass concentrated on top of the beam. They studied and controlled the beam based on Euler-Bernoulli theory analytically and numerically. In addition to optimal placement, they optimized the size of piezoelectric sensor and actuator in this model and their controlling method was done by using Lyapunov function [22].

L. Nowak et al. proposed a method for calculating the optimal place of piezoelectric sensor and actuator. Thin beam, thin plate and thin panel were tested as structures with different boundary conditions under acoustic vibration. The dynamic analysis of structure was conducted analytically [23]. G. Rosi et al. controlled the inactive released sound on an aluminum plate with non-standard boundary conditions and by optimal placement on it; they considered coordinates for locating piezoelectric pieces. Generally the objective was reaching the best efficiency of this plate in reducing the released sound from it [24].

A.H. Daraji et al. used an isotropic cantilever plate through finite element method in ANSYS software by using 2 elements; element Solid45 for 3D meshing and element Shell63 for 2D meshing of plate. They also used element Solid45 for meshing piezoelectric sensor and actuator pieces and prepared the model for controlling and by using Linear Quadratic performance index (minimization) and genetic algorithm in MATLAB software, they were able to relate these two software simultaneously in order to accelerate the vibration suppression through the optimal placement of piezoelectric pieces and showed their results [25]. J.M. Hale studied their placement by 10 piezoelectric pieces as sensors and actuators on a cantilever plate. They used genetic algorithm for optimization of objective function. Modeling method was in accord with first order shear theory and was conducted numerically by finite element and Hamilton relationship. Their objective for optimal placement was reaching the damping of first 6 vibrational modes of plate which were implemented analytically by ANSYS software by using element Solid45 for 3D meshing and element Shell63 for 2D meshing of plate and compared their results with finite element method.

Optimized objective function was modified by H2 soft in genetic algorithm to find the optimal place [26]. Nemanja D. Zoric et al. tried to optimized the size and location of piezoelectric on a thin composite beam by modeling finite elements based on the third order shear deformation theory, using fuzzy logic combination and PSO optimization algorithm with the swarm of one objective particles[27].

Sergio L. Schulz et al. used piezoelectric pieces for the optimal location on a cantilever beam and a plate with simply support. Their optimization method was genetic binary algorithm and Linear Quadratic Gauss (LQG) method. In this study, their optimization objective function was designed based on Lyapunov function. During this research, they reached to this goal that optimal location in many first modes that are considered as energetic modes can control the system and cover other vibration modes. State variables, kinetic energy, strain energy and input voltage of actuator are considered and considerable results were provided [28].

D. Chhabra et al. in their article optimally located 10 piezoelectric actuators on a square plate with simply support by using Modified Control Matrix and Singular Value Decomposition (MCSVD) method and genetic algorithm and finally for vibration control, they used LQR controlling rule in order to investigate the performance and efficiency of system and this way, they optimized and controlled first 6 vibration modes in square plate [29].

F. Botta et al. suggested a new objective function for optimal locating of piezoelectric. Optimization of the objective function results in simultaneously damping of several vibration modes. Heir studied structure was a cantilever beam with using Euler-Bernoulli theory. Their modeling of beam was done in two ways; analytically and numerically and showed the conformity of these two methods. Also in another article, they obtained experimental results from optimal placement of piezoelectric as sensor and actuator on turbo machinery blades. They considered a turbo machinery blade as a cantilever beam and then analytically solved the equation of beam coupled with piezoelectric sensor and actuator and presented their theoretical and experimental results.

Their objective was to reduce vibration and fatigue of the beam [30]. A.L. Araujo et al. conducted the optimal placement of piezoelectric on a Sandwich plate with viscoelastic core and multi-layered procedure by using DMM optimization method. Because of this research, they were able to analyze the vibration suppression of sandwich plate by finding the best place and by analyzing 6 vibration modes. They found considerable results [31]. S. Wrona et al. in two different articles used local directional controllability theory to find the optimal place for piezoelectric sensor and actuator. Their studied structure was isotropic square plate with four sides clamped. They used Memetic algorithm to optimize the controllability index. Memetic algorithm has a proper performance due to faster convergence and better statistical solution [32-33]. A.Takezawa et al. proposed an optimization methodology for piezoelectric sensor and actuator for vibration control truss structure based on numerical method optimization [34]. W.Dafang et al. experimental studied about beam structure by using patch piezoelectric and for comparison experimental and analytical method was used the independent modal space method [35].

F.M.Li and X.X.Lv investigated vibration control of lattice sandwich beam using the sensor and actuator piezo-patch and designing controller with the velocity feedback control method and linear quadratic regulator for suppressing lattice sandwich beam displacements [36]. M.K.Kwak and D.H.Yang investigated fluid structure interaction (FSI) in rectangular plate structure submerged in a fluid for analyzing active vibration control piezo-structure and for controlling system. They used MIMO (Multi- Input Multi-Output) positive position feedback controller [37]. K.Khorshidi et al. in their studies which is controlled circular plates coupled with piezoelectric layers excited by plane sound wave based on classical plate theory and using LQR and Fuzzy-Logic controllers [34].

M.A.Trindade et al. designed semi-model active vibration control of plate structure and using modal filter with distribution piezoelectric patches on structure [38]. S.Q.Zhang et al. using various nonlinearities method for designing vibration suppression composite thin-walled structure with 2 types laminated such as cross-ply and angle-ply. They used negative proportional velocity feedback control and piezoelectric material for reducing vibration structure [39]. K.Yildirim and I.Kucuk designed optional controller for vibration attenuation simply-supported Timoshenko beam by using piezoelectric [37]. B.A.Selim et al. in their study that could investigated to active vibration control of functionally graded material (FGM) plate and using Reddy's higher-order shear deformation theory (HSDT) and implemented piezo-Layers for reducing vibration stricture [40].
O.Abdeljaber et al. discussed neurocontroller for active vibration control cantilever plate for designing optimal voltage piezoelectric actuator by using neural network [38]. J. Plattenburg et al. investigated vibration control cylindrical shell with piezo-patches and distributed cardboard liner [41]. B.A.Selim et al. designed CNT-reinforced composite plates and cylindrical shells with Reddy's higher shear deformation and using piezoelectric layers [42]. In this study structure is a beam with cantilever boundary condition whose constitutive equations have been extracted by numerical method if finite element based on Timoshenko theory. Timoshenko theory shows more accurate behavior compared to Euler-Bernoulli beam because of shear effect during transformation.
Then, piezoelectric patches are installed in an optimal place as a sensor and actuator with given number through finite elements and beam division to given elements. This optimal location has been determined by MOPSO with considering two targets, i.e. maximum transverse displacement and reduced suppression time. Finally, LQR controller, which is a connector, is used between sensor and actuator. The signals are received from sensor and the best signal of voltage is applied on piezo actuator so that it can have a good vibration control.

2 Modeling Structure

2-1 Timoshenko Beam Constitutive Equations

A cantilever beam with rectangular cross-section with following dimensions is assumed (Figure 1).
For dynamic model of the structure of this beam and describing the beam with determined conditions, mass, stiffness, damping, and force matrices should be used. However, to describe the matrices, several steps of modeling and calculations by numerical method of finite element formulation would be done, which are as follows:

1) Describing meshing type of the beam
2) Extracting shape function matrix to describe each node
3) Extracting the relation between potential energy, kinetic energy and virtual work
4) Extracting the relations of obtaining mass, stiffness, and force matrices
5) Using shape function matrix in step 4
6) Obtaining mass, stiffness, and force matrices for one element from step 5
7) Using Rayleigh-Ritz relation to obtain damping matrix using step 6
8) Assembling the piezoelectric sensor and actuator on the structure
9) Performing simulations using Newton's second law and state space method

Timoshenko beam is a beam designed based on Timoshenko theory in 1921 that has covered the failure of Euler- Bernoulli beam. Timoshenko beam unlike Euler- Bernoulli beam after deformation remains perpendicular to neutral axis, but this is not assumed in Euler- Bernoulli beam. Timoshenko beam considers shear effect during deformation, as can be seen. This beam has provided a more real model during deformation.

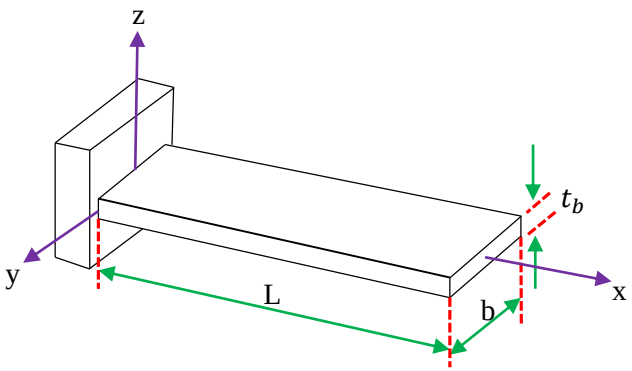

Figure 1 Cantilever Beam with Rectangular Cross-Section

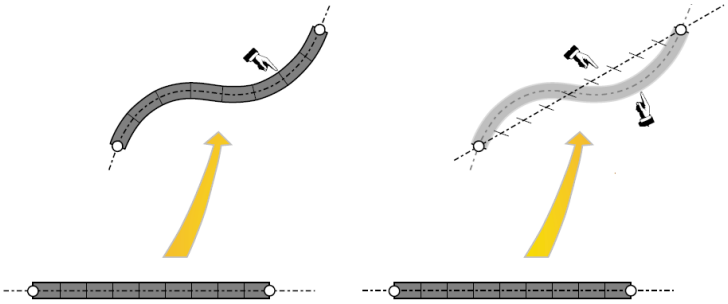

Figure 2 Shearing Effects in Timoshenko Beam

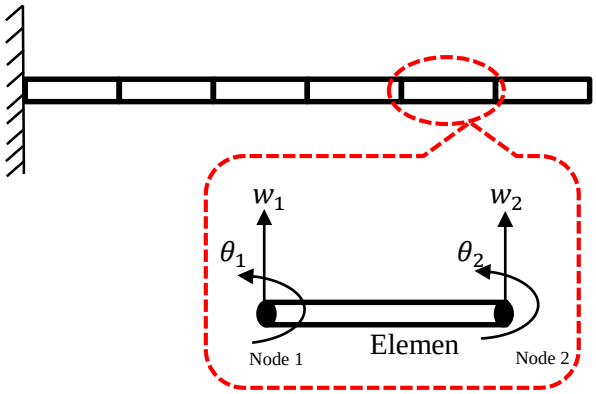

Figure 3 Degree of Freedom for every Node of Elements

In order to mesh the beam, the beam is first divided into nodes. Then, 2 degree of freedom is assumed for each node:
Now, it is assumed that w and θ are transverse and angular displacements, respectively, and are a function of beam length based on the following equation:

$$\omega = a_0 + a_1 x + a_2 x^2 + a_3 x^3 \quad (1)$$

$$\theta = b_0 + b_1 x + b_2 x^2 \quad (2)$$

Now, using BC's of cantilever beam and applying it on equations (1) and (2), shape function matrix for a Timoshenko beam is extracted as follows[47].

$$[\mathrm{N_w}]^{\mathrm{T}} = \frac{1}{1+\varphi}\begin{bmatrix} 2\left(\frac{\mathrm{x}}{l_e}\right)^3 - 3\left(\frac{\mathrm{x}}{l_e}\right)^2 - \varphi\left(\frac{\mathrm{x}}{l_e}\right) + 1 + \varphi \\ \left(\frac{\mathrm{x}}{l_e}\right)^3 - (2+\frac{\varphi}{2})\left(\frac{\mathrm{x}}{l_e}\right)^2 - (1+\frac{\varphi}{2})\left(\frac{\mathrm{x}}{l_e}\right) \\ 2\left(\frac{\mathrm{x}}{l_e}\right)^3 - 3\left(\frac{\mathrm{x}}{l_e}\right)^2 - \varphi\left(\frac{\mathrm{x}}{l_e}\right) \\ \left(\frac{\mathrm{x}}{l_e}\right)^3 - (1-\frac{\varphi}{2})\left(\frac{\mathrm{x}}{l_e}\right)^2 - \frac{\varphi}{2}\left(\frac{\mathrm{x}}{l_e}\right) \end{bmatrix} \tag{3}$$

Where, N_w is in fact the relation between local displacement and global displacement w(x, t) of the beam.

$$\mathrm{w(x,t)} = \mathrm{N_w q} \tag{4}$$

Where, w(x, t) describes transverse displacement of each element in global state. In order to find angular displacement of an element in global state:

$$\theta(x,t) = \left[\frac{\partial N_w}{\partial x}\right] q = N_\theta q \tag{5}$$

For a Timoshenko beam, potential energy, kinetic energy, and virtual work equation is described as follows [47]:

Potential energy:

$$U = \frac{1}{2}\int_0^{l_e} \begin{bmatrix} \frac{\partial\theta(x,t)}{\partial x} \\ \frac{\partial w(x,t)}{\partial x} + \theta(x,t) \end{bmatrix}^T \begin{bmatrix} EI & 0 \\ 0 & KAG \end{bmatrix} \begin{bmatrix} \frac{\partial\theta(x,t)}{\partial x} \\ \frac{\partial w(x,t)}{\partial x} + \theta(x,t) \end{bmatrix} dx \tag{6}$$

Kinetic energy:

$$T = \frac{1}{2}\int_0^{l_e} \begin{bmatrix} \frac{\partial w(x,t)}{\partial t} \\ \frac{\partial\theta(x,t)}{\partial t} \end{bmatrix}^T \begin{bmatrix} \rho A & 0 \\ 0 & \rho I \end{bmatrix} \begin{bmatrix} \frac{\partial w(x,t)}{\partial t} \\ \frac{\partial\theta(x,t)}{\partial t} \end{bmatrix} dx \tag{7}$$

Virtual work:

Each equation consists of transverse and angular displacement. Now, equations 4 and 5 are

$$\mathrm{W_v} = \int_0^{l_e} \begin{bmatrix} \mathrm{w(x,t)} \\ \theta(\mathrm{x,t}) \end{bmatrix}^{\mathrm{T}} \begin{bmatrix} \mathrm{f} \\ \mathrm{m} \end{bmatrix} \mathrm{dx} \tag{8}$$

placed in equations 6, 7, and 8. For mass and stiffness matrices, an element of the beam due to considering transverse and angular displacement in the node a stiffness and mass matrix is extracted for transverse displacement and stiffness and mass matrix is extracted for angular displacement. Therefore, for mass matrix using equation 9 in two parts, equation 10 that consists of mass matrix for transverse and angular displacement is presented.

$$\mathrm{M_s} = \int_0^{l_e} \begin{bmatrix}[\mathrm{N_w}]\\ [\mathrm{N_\theta}]\end{bmatrix}^{\mathrm{T}} \begin{bmatrix}\rho\mathrm{A} & 0\\ 0 & \rho\mathrm{I}\end{bmatrix} \begin{bmatrix}[\mathrm{N_w}]\\ [\mathrm{N_\theta}]\end{bmatrix} \mathrm{dx} \tag{9}$$

$$\mathrm{M_s} = \mathrm{M_w} + \mathrm{M_\theta} \tag{10}$$

Mass matrix for transverse displacement [47]:

$$\mathrm{M_w} = \rho\mathrm{A} \int_0^{l_e} [\mathrm{N_w}]^{\mathrm{T}} [\mathrm{N_w}] \mathrm{dx} \tag{11}$$

Mass matrix for angular displacement:

$$\mathrm{M_\theta} = \rho\mathrm{I} \int_0^{\mathrm{l_e}} [\mathrm{N_\theta}]^{\mathrm{T}} [\mathrm{N_\theta}] \mathrm{dx} \tag{13}$$

As a result beam mass matrix is:

$$M_{beam} = M_w + M_\theta \tag{15}$$

Similar to the process of achieving mass matrix, stiffness matrix is also divided into two parts. One is related to transverse displacement and the other is related to angular mass. Equation 16 is defined and is stated as equation 17 [47].

$$[\mathrm{K_s}] = \int_0^{l_e} \begin{bmatrix} \dfrac{\partial}{\partial \mathrm{x}}[\mathrm{N_\theta}] \\ [\mathrm{N_\theta}] + \dfrac{\partial}{\partial \mathrm{x}}[\mathrm{N_w}] \end{bmatrix}^{\mathrm{T}} \begin{bmatrix}\mathrm{EI} & 0\\ 0 & \mathrm{KGA}\end{bmatrix} \begin{bmatrix} \dfrac{\partial}{\partial}[\mathrm{N_\theta}] \\ [\mathrm{N_\theta}] + \dfrac{\partial}{\partial}[\mathrm{N_w}] \end{bmatrix} \mathrm{dx} \tag{16}$$

$$\mathrm{K_s} = \mathrm{K_w} + \mathrm{K_\theta} \tag{17}$$

Stiffness matrix for an element in the transverse displacement is extracted from equation 16.

$$\mathrm{K_w} = \mathrm{EI} \int_0^{l_e} \left[\frac{\partial \mathrm{N_\theta}}{\partial \mathrm{x}}\right]^{\mathrm{T}} \left[\frac{\partial \mathrm{N_\theta}}{\partial \mathrm{x}}\right] \mathrm{dx} \tag{18}$$

Similarly, stiffness matrix of angular displacement is obtained from equation 16.

$$\mathrm{K_\theta} = \mathrm{KGA} \int_0^{l_e} \left[\mathrm{N_\theta} + \frac{\partial \mathrm{N_w}}{\partial \mathrm{x}}\right]^{\mathrm{T}} \left[\mathrm{N_\theta} + \frac{\partial \mathrm{N_w}}{\partial \mathrm{x}}\right] \mathrm{dx} \tag{19}$$

In the obtained mass and stiffness matrices (equations 12, 14, 20, 21), φ is expressed as shear coefficient parameter that is expressed depending on the type of beam cross section.

$$\varphi = \frac{24}{{l_e}^2}\left(\frac{1}{KA}\right)(1+\nu) \tag{22}$$

Generally, shear coefficient for rectangular and circular cross-section is considered as follows [48].

Rectangle: $K = \frac{5}{6}$ Circular: $K = \frac{9}{10}$

As a result beam stiffness matrix is:

$$K_{beam} = K_w + K_\theta \tag{23}$$

Finally, the virtual work expresses the amount of force for an element as follows [47].

$$\mathrm{F} = \int_0^{l_e} \begin{bmatrix} \mathrm{N_w} \\ \mathrm{N_\theta} \end{bmatrix}^{\mathrm{T}} \begin{bmatrix} \mathrm{f} \\ \mathrm{m} \end{bmatrix} \mathrm{dx} \tag{24}$$

3 Smart Materials

Due to their special characteristics, smart materials receive different environmental conditions such as stress fields, heat, magnetism, and electricity, and react to them. Depending on the properties of these materials, these materials are used as sensors or actuators in various sectors. Smart materials along with control systems and structures such as beam, plate, and shell comprise smart structures. These structures using sensors made from smart materials receive conditions and changes from the environment and actuators receive control effort signal controller for controlling structure. Shape memory alloys, smart fluids, magnetostrictive and electrostrictive materials, and piezoelectric materials are a class of smart materials.

3-1 Linear Piezoelectric Constitutive Equation

Piezoelectric effect states direct and inverse electromechanical coupling. Direct effect is producing electric charge as a result of mechanical stress to piezoelectric material. Adverse effect is mechanical deformation when placing piezoelectric material in an electric field. For linear piezoelectric material, according to Ref. [49] equations (25) and (26) that are called fundamental equation, the relationship between mechanical and electrical variables is expressed.

$$\sigma = \mathrm{c^E S} - \mathrm{e^T E}^p \tag{25}$$

$$\mathrm{D} = \mathrm{eS} + \varepsilon^{\mathrm{S}} \mathrm{E}^p \tag{26}$$

Where, σ is mechanical stress, D is charge density (per unit area), S is mechanical strain, c^E is mechanical stiffness, e is piezoelectric strain constant, E^p is electric field of piezoelectric and ε^s is electric permittivity. Superscripts S and E^p indicate the measured values in the constant electric field and constant strain. Equation (25) represents the inverse piezoelectric effect, and equation (26) shows the direct piezoelectric effect. Using the direct effect, piezoelectric material can convert different mechanical deformations into electrical charges, so it can act as a sensor. In contrast, piezoelectric material can cause mechanical deformation by receiving electrical voltage, so it can be used as a stimulant.

Due to simultaneous direct and reverse effects, piezoelectric materials can simultaneously without significant change in stiffness or weight of the systems stick on their surface and work in conjunction with these systems.

3-2-1 PZT Model

In this model, the target of optimal location or optimal placement is a pair of piezoelectric sensor and actuator elements on a cantilever beam. A beam with the stated dimensions is divided into 20 elements, so that the size of each beam element is equal to the length of piezoelectric patch. Now, with LQR controller and MOPSO algorithm under alternating inputs it has been tried to find the optimal location for vibration suppression. Figure (4) schematically shows 1PZT Model in which the length of each element of the beam is equal to piezoelectric sensor and actuator. By dividing the length of the beam element into 20 equal elements, optimal displacement of piezoelectric patches on the top and bottom of the beam is done. Vibration is prevented and the structure is attenuated. Figure (4) shows the control system for 1PZT Model in real-mode and laboratory. A/D and D/A blocks are convertors that convert signals from analog to digital and digital to analog, respectively, so that a relationship is established between sensor and actuator with the controller (computer). Amplifier block is a constant magnification.

3-3-5 PZT Model

Research conducted in the field of optimal placement of piezoelectric element in the last decade were mostly done on a pair of piezoelectric patches or a given number of piezoelectric elements, but with no reduction in piezoelectric element size or in other words however, in 5PZT Model, the 1PZT Model is actually considered with slight changes. That means a pair of piezo patches with reduced length of beam and dividing the piezo element into 5 smaller elements have been able to find optimal location. First, the beam in 1PZT Model is divided from 20 to 100 elements. In addition, the pair of piezoelectric patches are divided into 5 equal elements with beam length (100-element beam). It is aimed to find more optimal locations and more accurate points to locate piezo element that leads to vibration attenuation of the beam. Now, the system is controlled under subsequent inputs of LQR controller. Figure (5) shows 5PZT Model by dividing the beam length into 100 equal elements and dividing a piezoelectric path into 5 smaller patches in 1PZT Model.

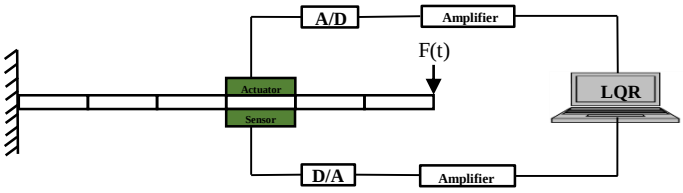

Figure 4 1PZT Model

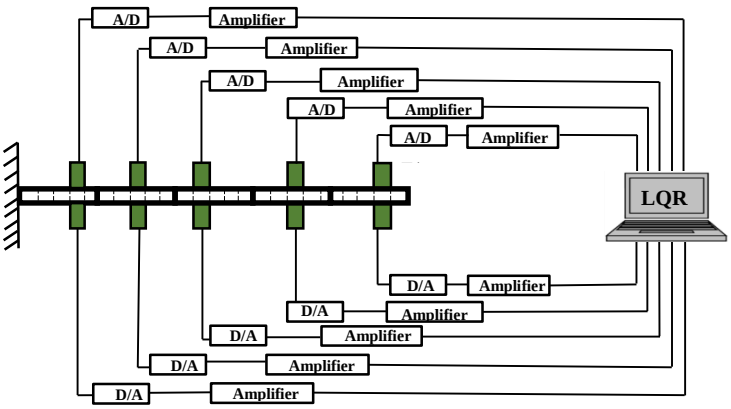

Figure 5 5PZT Model

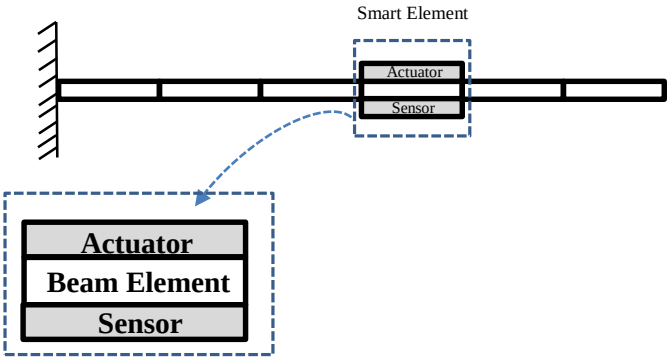

Figure 6 Smart Element of Beam

3-3 Assemblage Beam with Sensor and Actuator

Assume the following cantilever beam with a pair of piezoelectric elements as a sensor and actuator embedded at the bottom and top of the beam, respectively.

$$M_{SE} = M_{be} + 2M_p \tag{27}$$

$$K_{SE} = K_{be} + 2K_p \tag{28}$$

Equations 27 and 28 are stiffness and mass matrices for an element of the beam on which piezoelectric sensor and actuator patches are embedded. If after assembling the piezoelectric patches were deployed with the structure through elimination method in definite element, stiffness and mass matrices will be achieved for a smart structure in equations 29 and 30.

$$M_{smart} = Assamblge(M_{beam}, \sum M_{SE}) \tag{29}$$

$$K_{smart} = Assamblge(K_{beam}, \sum K_{SE}) \tag{30}$$

Generally, equations 29 and 30 state mass and stiffness matrices of a structure in assembled mode. Then, dynamic stimulation for the structure is possible with these equations. Now, damping matrix of the system is obtained using equations 29 and 30 as Rayleigh-Ritz equation 31.

$$C_{smart} = \alpha M_{smart} + \beta K_{smart} \tag{31}$$

Where, $\boldsymbol{\alpha}$ and $\boldsymbol{\beta}$ are Rayleigh–Ritz coefficients obtained through laboratory testing on the smart structure. Using Newton's second law, we describe the dynamic of system and displacement, velocity, and acceleration extraction are discussed.

3-4 Benefits of Optimal Locations

Locating piezo-ceramic sensor and actuator has significant benefits, which we can note several of them. As can be seen in Figure (7-b), rather using a layer of sensor and actuator at the top and bottom of an engineering structure, patches of sensor and actuator are used, which leads to a series of unique features in structure control, including:

power saving, high accuracy, generating large power, less weight, greater sensitivity, reducing energy consumption, controlling more vibration modes.

(a) (b)

Figure 7 Type of Piezoelectric Materials (a) PVDF (b) PZT

4 Dynamic Formulation of Smart System

According to Newton's second law, dynamic behavior of a system can be modeled as equation 32.

$$M_{smart}\ddot{z} + C_{smart}\dot{z} + K_{smart}z = f_t \tag{32}$$

f_t consists of external force and control force applied by the piezoelectric actuator.

$$f_t = f_e + f_c \tag{33}$$

Voltage applied to the piezoelectric actuator V_a is applied using the signal sent from the controller of voltage and converting the voltage into analog and in fact, transition from digital to analog convertor. In piezo electro-mechanical system and beam, a voltage of piezo actuator should be defined on the beam as follows [47].

$$V_a = \left[K_c G_c e_{31} z b \int_0^{l_p} [N_a]^T dx\right] \dot{q} \tag{34}$$

Where

$$z = \frac{t_b}{2} + t_p \qquad \mathrm{N_a} = \frac{\partial \mathrm{N_\theta}}{\partial \mathrm{x}} \tag{35}$$

Where, control force generated by the piezoelectric actuator is considered as equation 36.

$$f_c = \left[E_p e_{31} b \bar{z} \int_0^{l_p} [N_\theta]^T \, dx\right] V_a \tag{36}$$

$\bar{z}$ is the distance between the natural beam axis and natural piezo-patch.

By describing a system as state space, a system with 2 inputs and multiple outputs is

$$\dot{\mathrm{z}} = \mathrm{A}_s \mathrm{z} + \mathrm{B}_s \mathrm{w(t)} + \mathrm{E}_{ce} \mathrm{u(t)} \tag{37}$$

Matrices used in state-space can be represented as equations 38-40.

$$\mathrm{A_s} = \begin{bmatrix} [0] & [\mathrm{I}] \\ -\left[\frac{\mathrm{K_{smart}}}{\mathrm{M_{smart}}}\right] & -\left[\frac{\mathrm{C_{smart}}}{\mathrm{M_{smart}}}\right] \end{bmatrix} \quad (38) \qquad \mathrm{B_s} = \begin{bmatrix} [0] \\ \left[\frac{\mathrm{f_e}}{\mathrm{M_{smart}}}\right] \end{bmatrix} \quad (39) \qquad \mathrm{E_{ce}} = \begin{bmatrix} [0] \\ \left[\frac{\mathrm{f_c}}{\mathrm{M_{smart}}}\right] \end{bmatrix} \quad (40)$$

To describe system output as equation 41, different views can be expressed so that Matrix C can be stated as:

$$\mathrm{y}_{out} = \mathrm{C}_s \mathrm{z} + \mathrm{D}_s \mathrm{u(t)} \tag{41}$$

1. Sensor voltage output should be considered [47].
2.

$$C_s = [[0] \quad [p]\,] \tag{42}$$

$$p = \left[G_c e_{31} z b \int_0^{l_p} N_a dx\right] \dot{q} \tag{43}$$

3. Displacement structure output should be considered.

$$C_s = [I] \tag{44}$$

On the other hand, matrix D in equation 41 is considered a null.

$$D_s = [0] \tag{45}$$

4-1 Optimization process

4-1-1 Multi-Objective Particle Swarm Optimization Algorithm (MOPSO)

Multi-Objective Particle Swarm Optimization Algorithm is a heuristic search that simulate the movements of a group of birds looking for food. Simplicity and being based on multi-objective have caused this method be a commonly used method in multi-objective optimization problems. To apply this method in multi-objective optimization problems, it is necessary to modify the single-objective algorithm of this method. While expanding the multi-objective Particle Swarm Optimization Algorithm, it is necessary to consider some questions [50]:

1. How the best group experience for each particle should be chosen? In other words, in what way should the particles be adopted among non-dominant solutions?
2. How non-dominant solutions should be maintained during the search process so that non-dominancy would be examined not only compared to previous population but also next population.
3. How can we have uniform and homogenous distribution from non-dominant points across Pareto Front? How can we maintain diversity in the population, so that the algorithm is not converging to one answer?

Position vector of i^{th} particle:

$$\vec{x}_i(t+1) = \vec{x}_i(t) + \vec{v}_i(t+1) \tag{46}$$

Velocity vector of i^{th} particle:

$$\vec{v}_i(t+1) = w_I\ \vec{v}_i(t) + C_1 r_1 \left(\vec{x}_{pbest_i}(t) - \vec{x}_i(t)\right) + C_2 r_2 \left(\vec{x}_{gbest}(t) - \vec{x}_i(t)\right) \tag{47}$$

$\vec{x}_{gbest}$ is storage repository of elite and non-dominant particles due to the optimization process. R_1 and r_2 are random values in [0, 1] and w is weight factor. C_1 and C_2 are individual learning and collaborative learning, respectively. By considering the references, optimal weights of 48^{th} and 53d equations have been adopted based on Ref. [51].

$$\phi_1 = \phi_2 = 2.05 \tag{48}$$

$$\phi = \phi_1 + \phi_2 \tag{49}$$

$$\chi = \frac{2}{\left(\phi - 2 + \sqrt{\phi^2 - 4\phi}\right)} \tag{50}$$

$$w_p = \chi \tag{51}$$

$$C_1 = \chi\phi_1 \tag{52}$$

$$C_2 = \chi\phi_2 \tag{53}$$

4-2 LQR Controller

4-2-1 Q & R Weighted Matrices

In Q and R matrices, 3 weighting coefficients are stated. The coefficients are discovered as search design variables by optimization algorithm and their optimal amount is found. Therefore, Q and R matrices are assumed as [17]. The defined intervals for α_1,α_2, and γ decide experimentally and are also obtained by trial and error.

4-3 LQR-MOPSO Controller

The objective function used in the optimization consists of 4 design variables, including:

1. The location of piezoelectric sensor and actuator patches
2. Three weighted coefficient matrices of Q and R in LQR controller, including α_1, α_2 and γ [14].

$$Q = \begin{bmatrix} \alpha_1[w_i{}^2] & [0] \\ [0] & \alpha_2[I] \end{bmatrix} \qquad R = \gamma[I] \tag{54}$$

Therefore, the objective function used in the MOPSO optimization algorithm can be briefly described. The objective function of control system is considered as equation 55.

$$J = \int (z^T Q z + u^T R u) dt \tag{55}$$

For J to be minimum in equation 55, its derivative with respect to time should be zero. So we have:

$$\frac{dJ}{dt} = z^T Q z + u^T R u = 0 \tag{56}$$

State variable vector x that contains the displacement and velocity of the system is defined as equation 57.

$$z = \begin{bmatrix} \eta \\ \dot{\eta} \end{bmatrix} \tag{57}$$

Control input for the system that is sent by LQR controller is considered as a function of state variables of the system as equation 58.

$$u = -K_{LQR} z \tag{58}$$

LQR controller gain is expressed as equation 59:

$$K = R^{-1} E^T P \tag{59}$$

Where, control gain of matrix E of state space and matrix P of Riccati equation (symmetric matrix) are respectively as equations 60.

$$P = \begin{bmatrix} P_{11} & P_{12} \\ P_{12} & P_{22} \end{bmatrix} \tag{60}$$

Now, by placing equations 54, 57, 58, 59, and 60 in two terms of $x^T Qx$ and $u^T Ru$ from equation 56, we have:

$$z^T Qz = \eta^T \alpha_1 w \eta + \dot{\eta}^T \alpha_2 \dot{\eta} \tag{61}$$

$$u^T Ru = \frac{1}{\gamma^3}\left[\frac{f_{ctrl}}{M}(P_{21}\eta + P_{22}\dot{\eta})\right]^T \left[\frac{f_{ctrl}}{M}(P_{12}\eta + P_{22}\dot{\eta})\right] \tag{62}$$

α_1,α_2, and γ are introduced to MOPSO in a given interval that can be obtained through trial and error. f_{ctrl} is related to control force of piezoelectric actuator in an optimal place. In order to apply control power in a place of the beam structure, the length of the beam should be introduced to the algorithm so that it would move the control power only along the beam length interval. Now, for better understanding of the piezoelectric element optimal location on the beam structure, a beam is schematically divided into 4 elements as Figure (8) and piezoelectric sensor and actuator element is placed on the third element of the beam. Each node of the beam element has 2 degrees of freedom (transverse and angular displacement).

On the other hand, productive behavior of the piezoelectric element is only angular displacement (torque). When the beam starts to vibrate, piezoelectric actuator patch in the third element reacts as torque to reduce fluctuations of the beam.

Now, if generating torque is described as force, in the previous section:

$$f_c = hV_a \tag{63}$$

Where, h is related to the place where piezoelectric element produces its torque [47].

$$h = E_{pzt} d_{31} b\bar{z} \int_0^{l_e} N_\theta \, dx \tag{64}$$

The voltage produced by the piezoelectric actuator element to produce mechanical behavior (torque) is also [47]:

$$V_a = K_{LQR} G_c d_{31} bz \int_0^{l_e} N_a \, dx \tag{65}$$

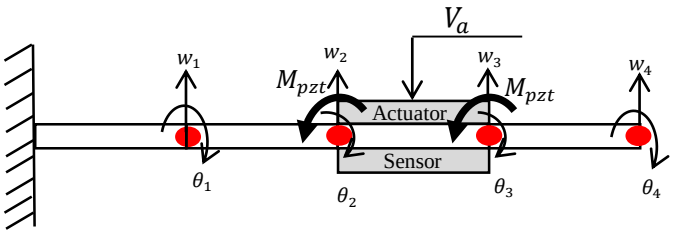

Figure 8 Schematic Smart Beam Model and Effects Piezo Patches

$$f_c = \begin{matrix} w_1 \\ \theta_1 \\ 3_2 \\ \theta_2 \\ w_3 \\ \theta_3 \\ w_4 \\ \theta_4 \end{matrix} \begin{bmatrix} 0 \\ 0 \\ 0 \\ E_{pzt} d_{31} b\bar{z} \\ 0 \\ E_{pzt} d_{31} b\bar{z} \\ 0 \\ 0 \end{bmatrix} V_a \tag{66}$$

Now, if we want to model equations 64 and 65 based on Figure (8), then it is placed in equation 63 and becomes in the form of equation 66. In 4th and 6th array in the matrix, equation 66 states the exact location based on Figure (8). MOPSO Algorithm will search and present the discovered location by dislocating the local non-zero entries (i.e. 4th and 6th array) that will have the most vibration attenuating effect.

5 Simulations Smart Beam

Simulation has been conducted on smart Timoshenko beam for 2 types of sequence inputs of step and impulse. In section 4, geometrical and mechanical characteristics of the beam and piezoelectric actuator and sensor patches are stated. Then, in sections 5, it has undergone step and impulse simulations and optimal location of piezoelectric sensor and actuator for 2 models of 1PZT and 5PZT.

5-1 Smart Timoshenko Beam

Table 1 Beam Information

Beam		
Symbol	**Parameters**	**Values**
L	Length	0.5 m
b_b	Width	0.024 m
E_b	Young's Modulus	193.096 GPa
ρ_b	Density	$\mathbf{8030}\ \frac{\boldsymbol{Kg}}{\boldsymbol{m^3}}$
α & β	Damping Constants	0.001 & 0.0001
t_b	Thickness	1 mm

Table 2 Piezo Patch Information [47]

PZT		
Symbol	**Parameters**	**Value**
l_{pzt}	Length	0.125 m
b_{pzt}	Width	0.024 m
t_{pzt}	Thickness	0.5 mm
E_{pzt}	Young's Modulus	68 GPa
ρ_{pzt}	Density	$\mathbf{7700}\ \frac{\boldsymbol{Kg}}{\boldsymbol{m^3}}$
d_{31}	Strain Constant	$\mathbf{125 \times 10^{-12}}\ \frac{\boldsymbol{m}}{\boldsymbol{V}}$
g_{31}	Stress Constant	$\mathbf{10.5 \times 10^{-13}}\ \frac{\boldsymbol{Vm}}{\boldsymbol{N}}$

Table 3 Natural Frequencies for 9 Modes in Timoshenko Beam

Natural Frequency (Hz)		
Analytical	**Numerical**	**ANSYS**
16.706	16.696	16.698
104.699	104.572	105.01
292.751	292.528	296.26
572.186	572.467	587.65
942.512	944.736	987.59
1402.112	1408.498	1506.4
1949.703	1962.947	2157.4
2584.256	2607.317	2957.5
3304.567	3340.965	3926.8

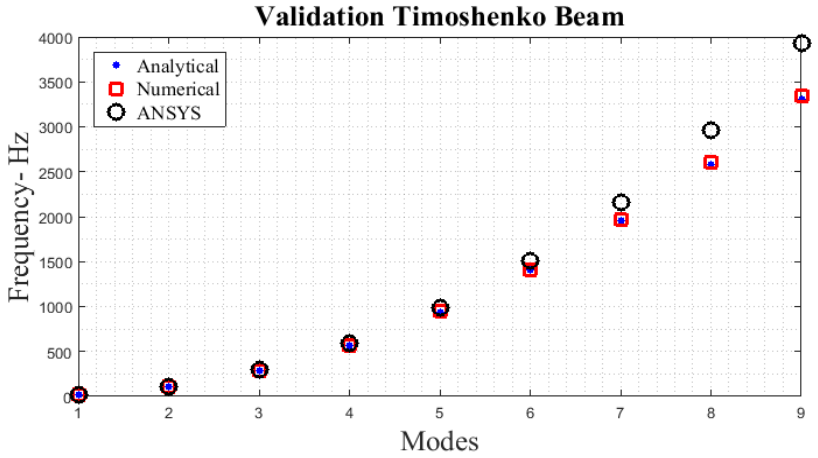

Figure 9 Camparison Naturel Frequencies of Timoshenko Beam

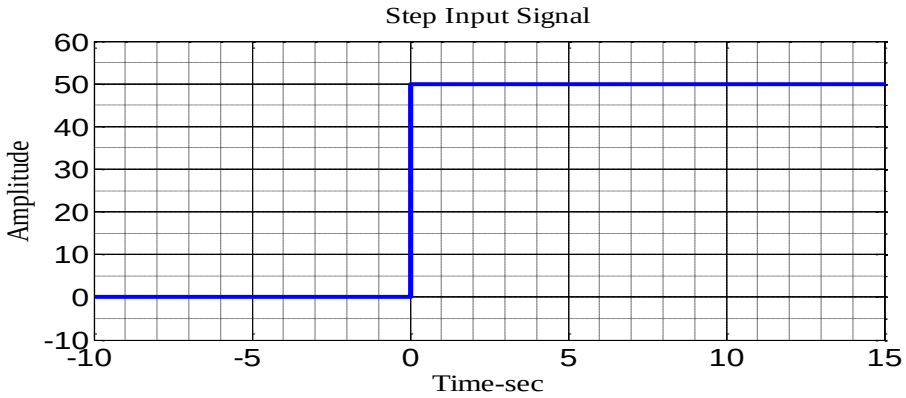

Figure 10 Step Input Value

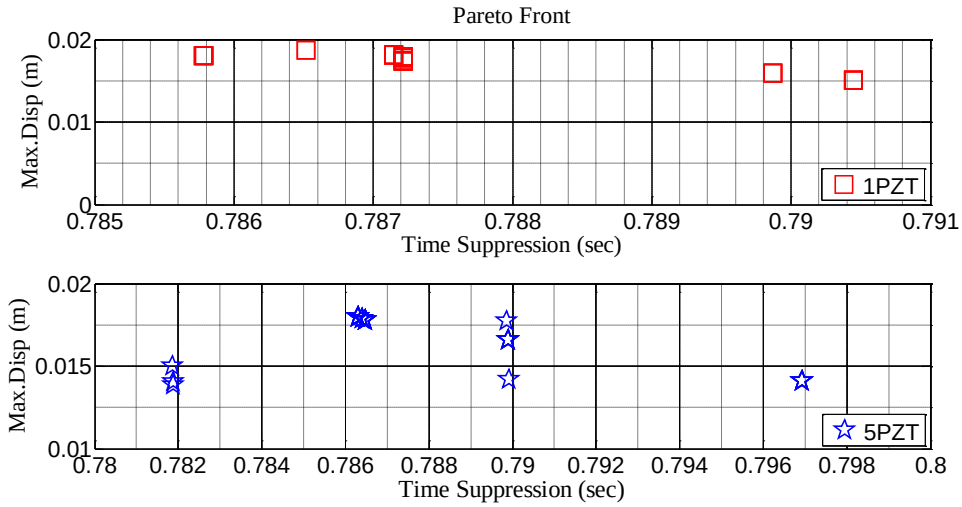

Figure 11 Step Input of Pareto Front

5-3 Step input

Step input for 1PZT and 5PZT control systems is shown in Figure (10).
In this input and Impulse input, two targets are placed for finding the standard optimum location. One is minimizing the attenuation time and the other is minimizing the maximum displacement of the structure (tip of the beam) against external stimulations. According to Figure (11), optimized Pareto Front of step input that is searched and discovered by MOPSO, the optimal points found by the algorithm had 2 objectives and satisfies both criteria.

Generally, the selection of one of the optimal points of Pareto in the two models is the responsibility of the designer and it is based on the needs and requirements of the design. Therefore, one of the points is displayed. In Figure (11), the transverse displacement of the beam tip for the two models, 1 pair of piezo and 5 pairs of piezo are shown as sensor and actuator due to step input. To be aware of the first seconds of input step effect on the beam, the horizontal axis (time axis) is plotted logarithmically, so that the effect of the two models is also learned in the first seconds.

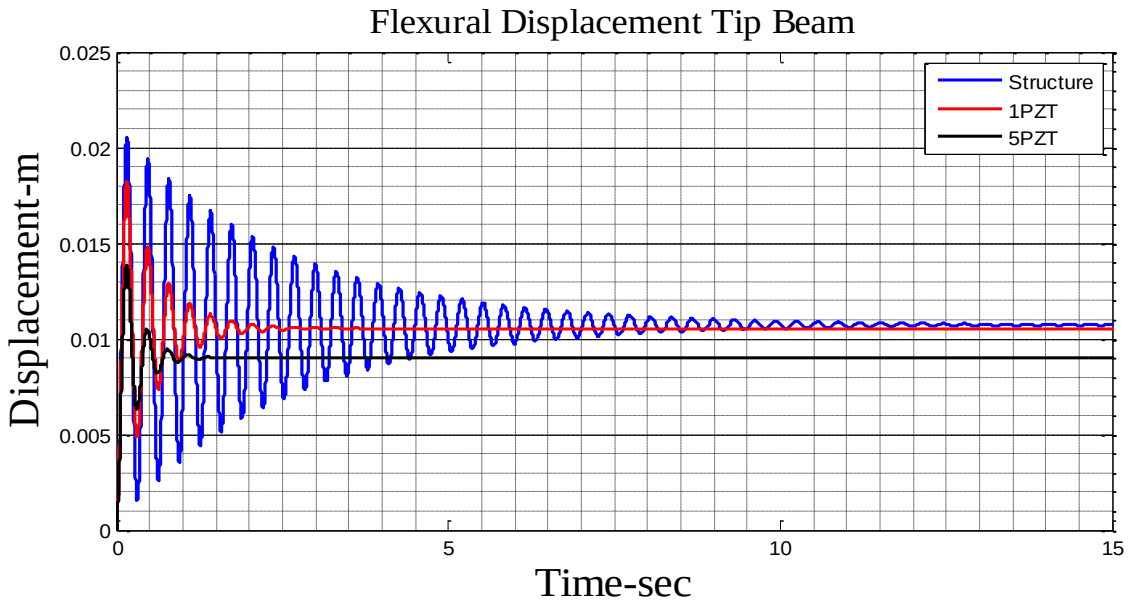

Figure 12 Step Flexural Displacement

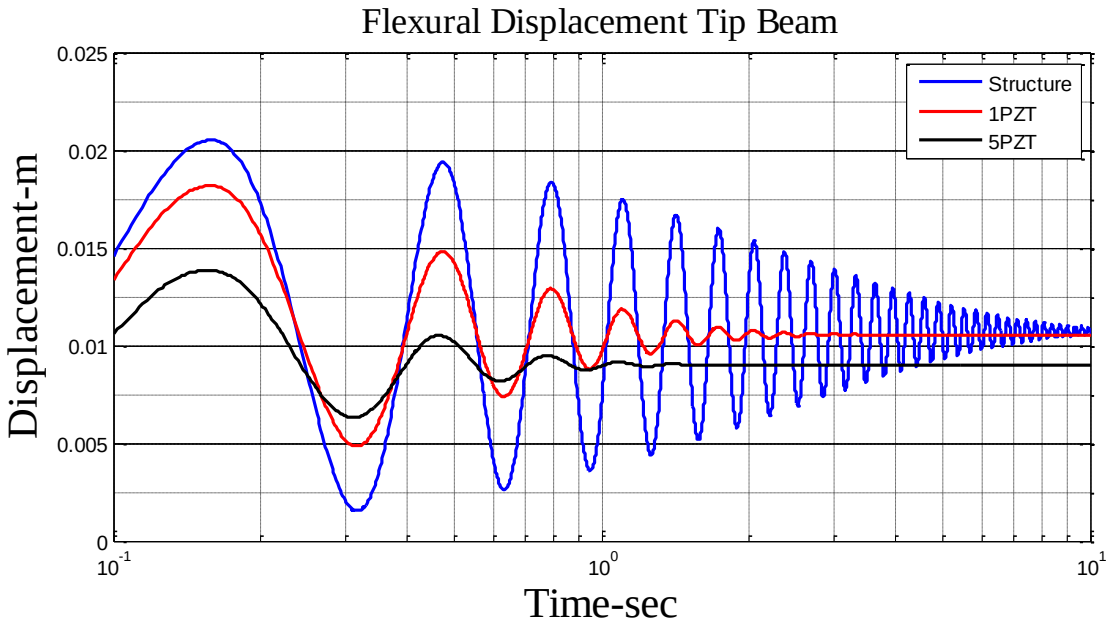

Figure 13 First Seconds Step Flexural Displacement

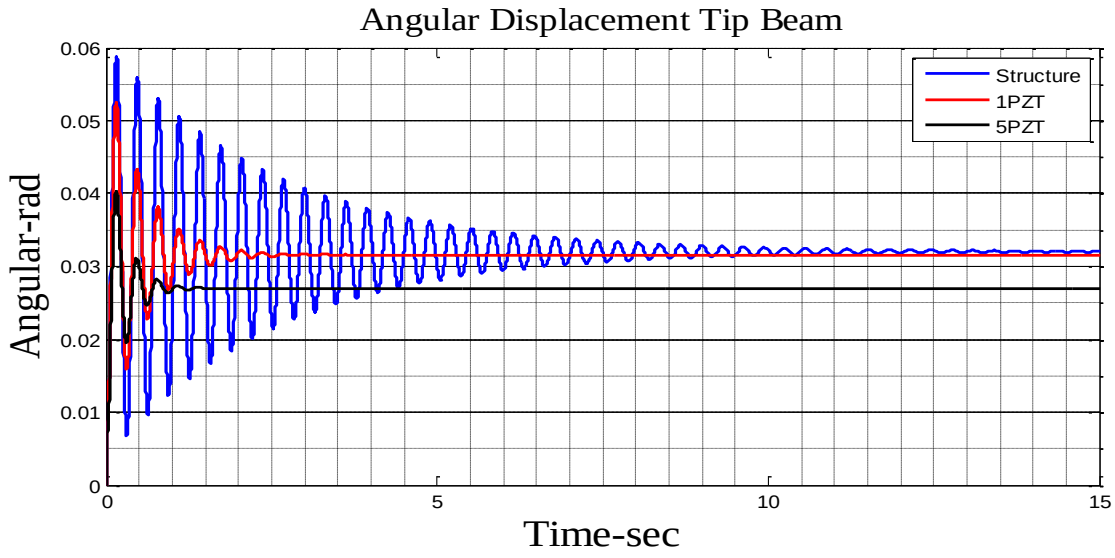

Figure 14 Step Angular Displacement

Angular movement for the beam tip for two models in the Step input is as follows. First seconds of step input on the beam where angular displacement of beam tip plotted logarithmically with the horizontal axis are as follows. Due to optimizing attenuation time and beam displacement, the piezoelectric actuator voltages in the models are as follows.

In this input and other leading inputs, the input voltages for the piezoelectric actuator placed as optimal values in interval control effort are shown [46].

Also, for the points selected from Pareto in Figure (10) have features that can be stated as attenuation time, maximum displacement, LQR controller coefficients, and optimal place of piezoelectric sensor and actuator in models 1PZT and 5PZT as shown in Table (4).
ces generated by the piezoelectric actuator for the models are shown in Figure (17).

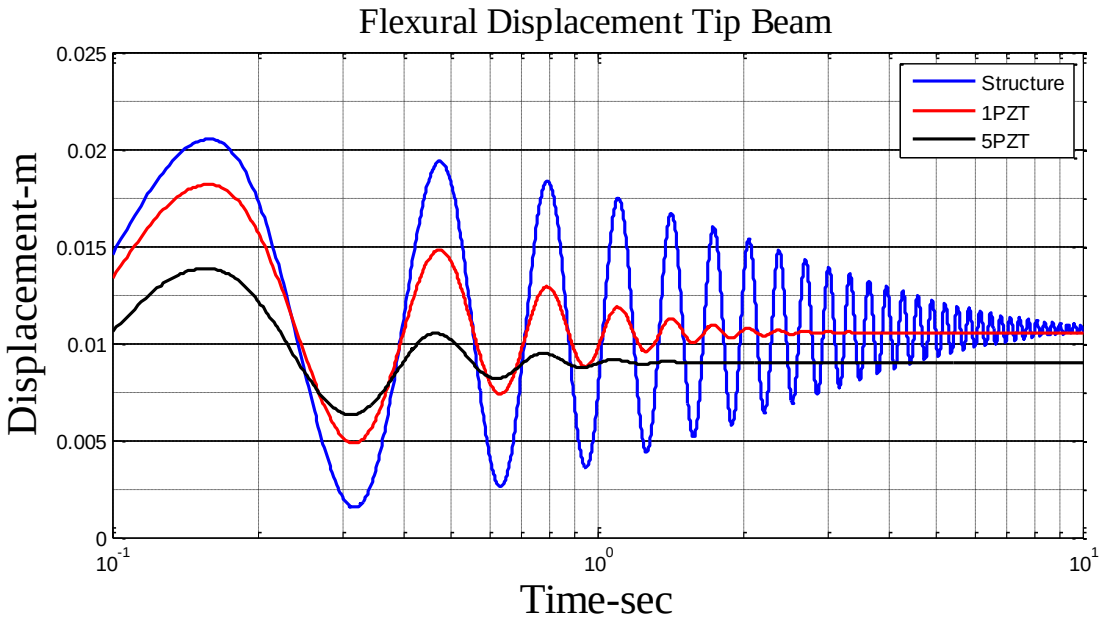

Figure 15 First Seconds Step Angular Displacement

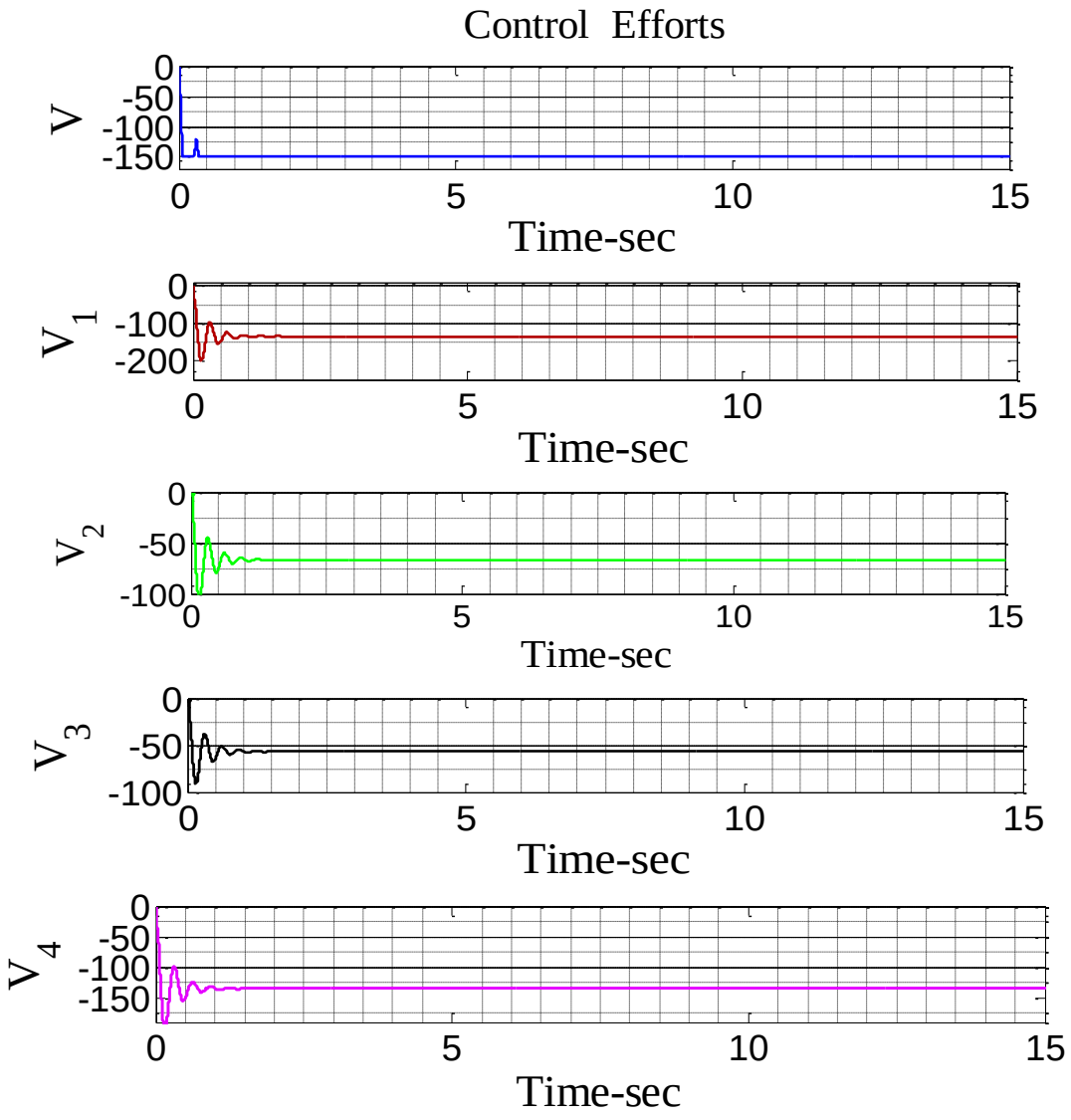

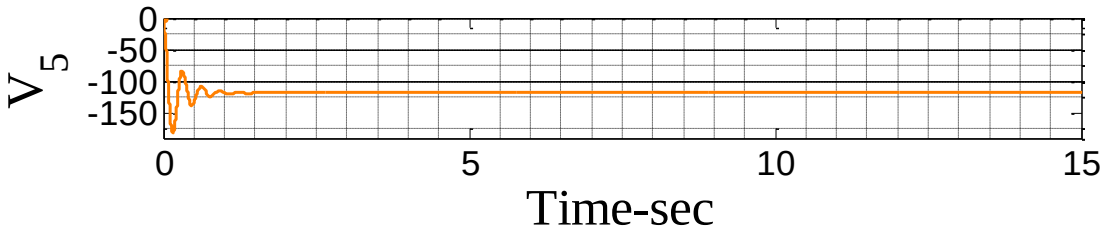

Figure 16 Step Voltage Actuators for 1PZT-5PZT Models

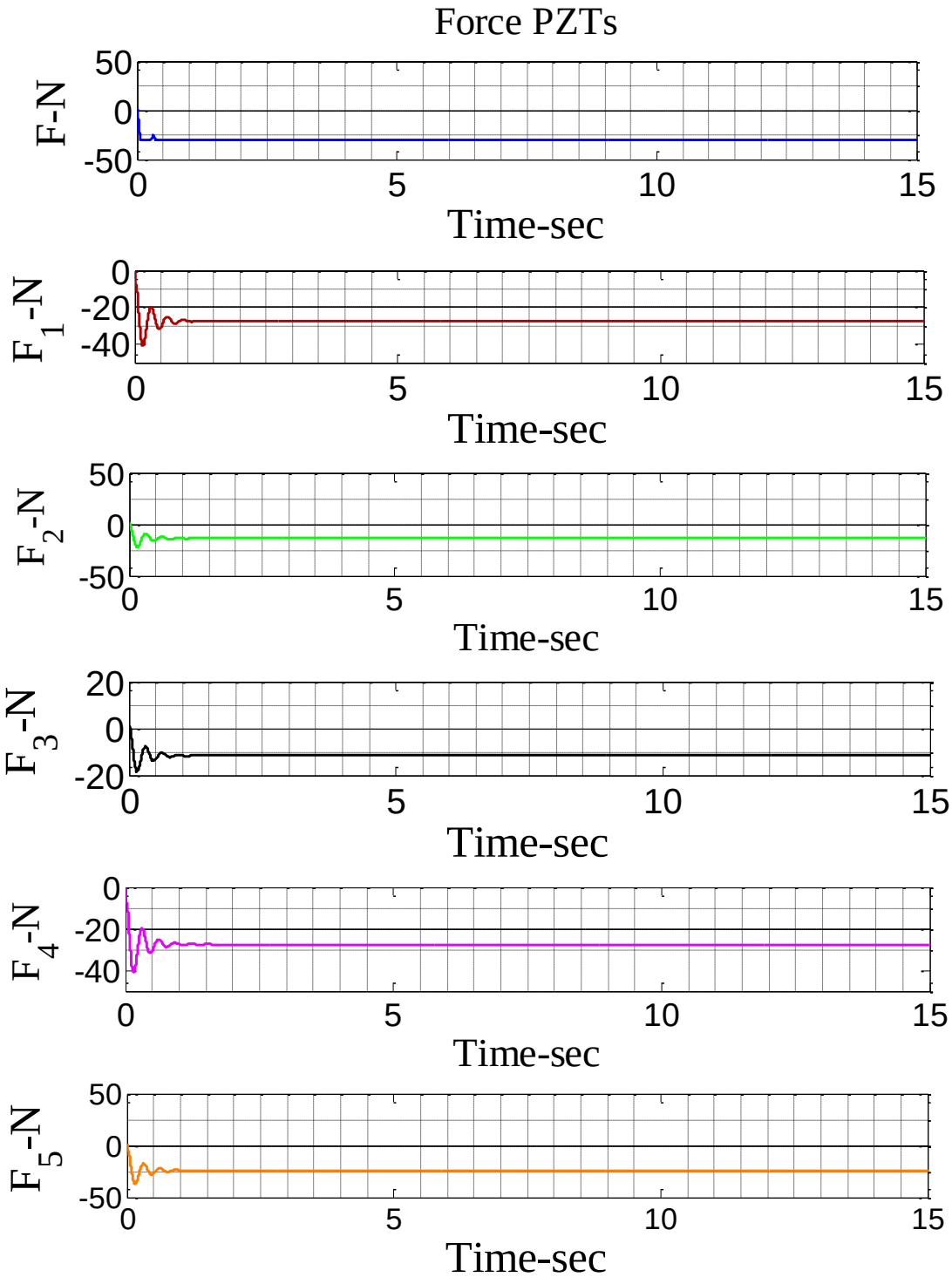

Figure 17 Step Force Actuators for 1PZT-5PZT Models

Table 4 Optimal Values of Impulse Input

		1 PZT	5 PZT
Objectives	Min.Time(sec)	0.7871	0.7818
	Max.Disp (m)	1.817×10^{-2}	$\mathbf{1.385 \times 10^{-2}}$
Element Location		12	[90,29,24,95,65]
LQR	α_1	95.3195	75.115
	α_2	82.191	10.938
	γ	0.256	0.0115

5-4 Impulse Input

Impulse input for 1PZT and 5PZT control systems are shown in Figure (18).

The Pareto Front extracted from the multi-objective particle swarm algorithm for impulse input for the two models is as follows.

Transverse displacement of the beam tip by applying impulse input on the beam in the models controlled by quadratic optimal controller is as follows. In this input, 5PZT proposed model presents a better response to structure attenuation than 1PZT.

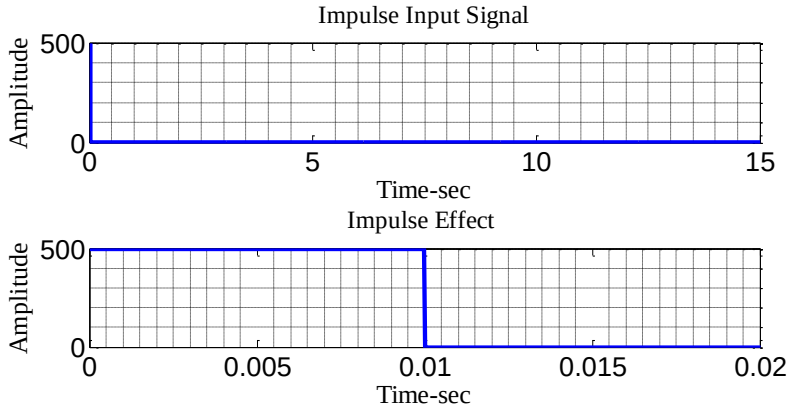

Figure 18 Impulse Input Value

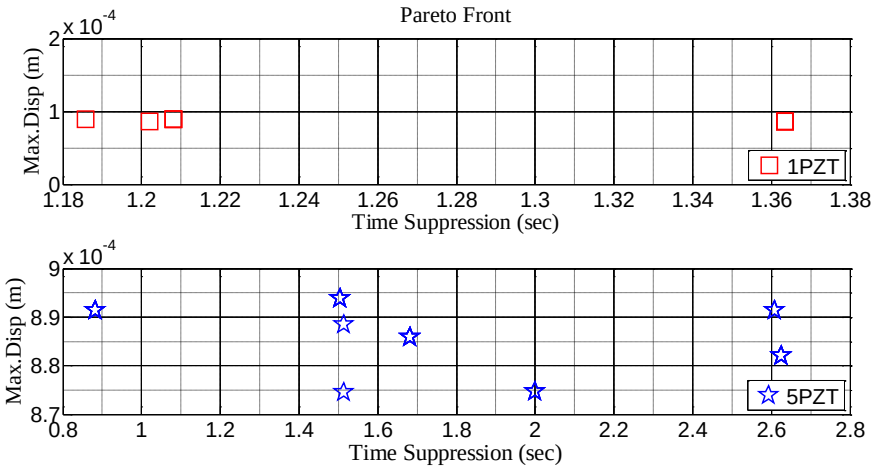

Figure 19 Impulse Input of Pareto Front

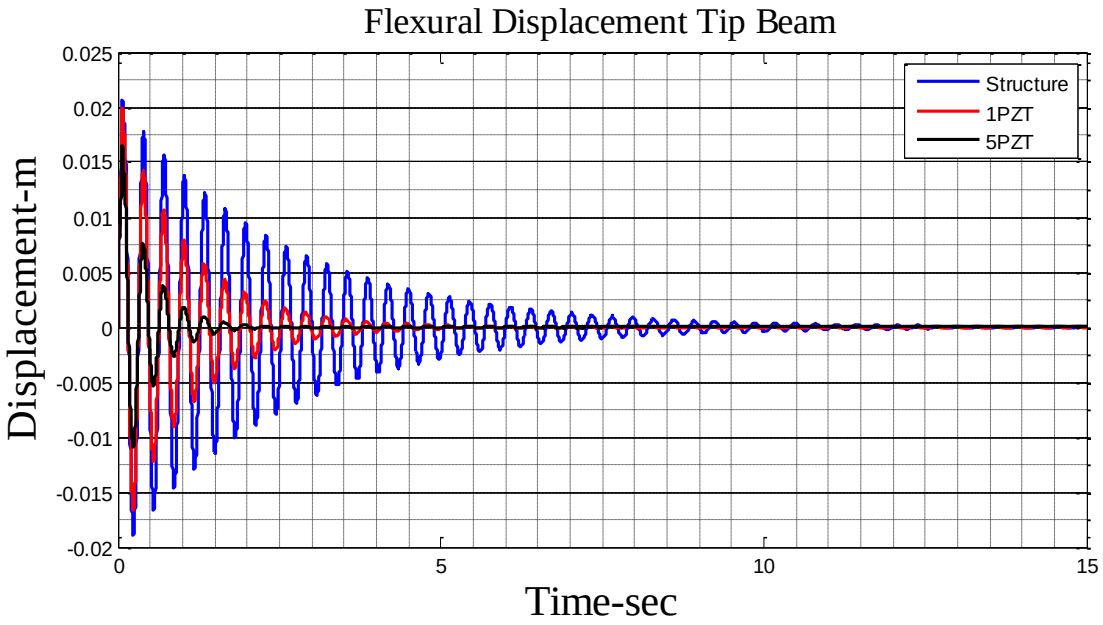

Figure 20 Impulse Flexural Displacement

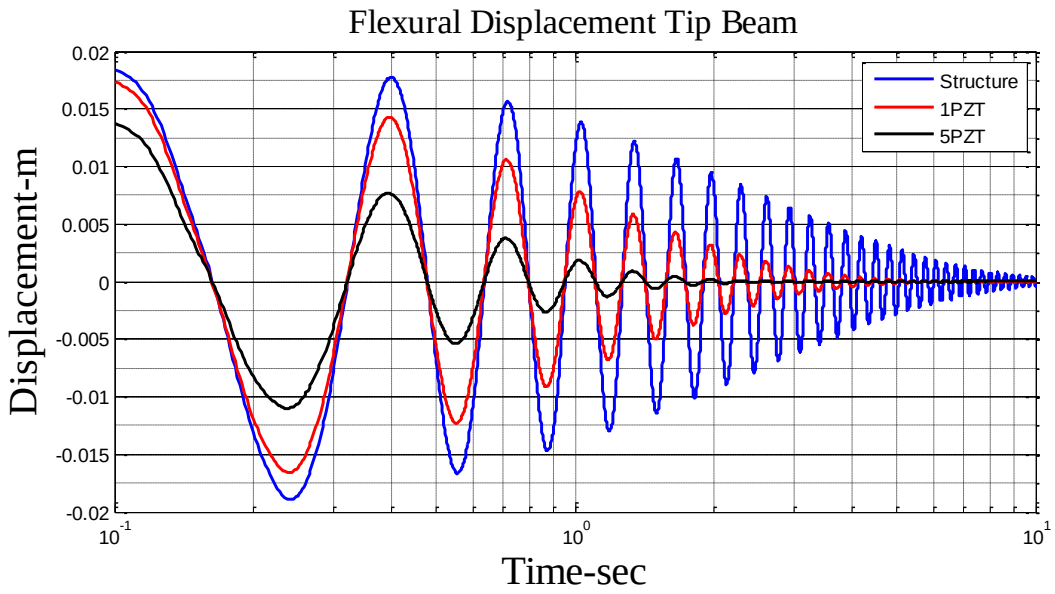

Figure 21 First Seconds Impulse Flexural Displacement

First seconds of impulse input in transverse displacement are displayed as follows.
Angular displacement of beam tip due to impulse input can be shown as follows.

By considering the horizontal axis as a logarithm, impulse input effect in angular displacement is as follows.

Information extracted from the optimal values of impulse input Pareto is as follows. Control effort of the piezoelectric actuators in the models in feasible piezoelectric range is as follows.

Also, forces generated by the piezoelectric actuators for the two models are as Figure (25).

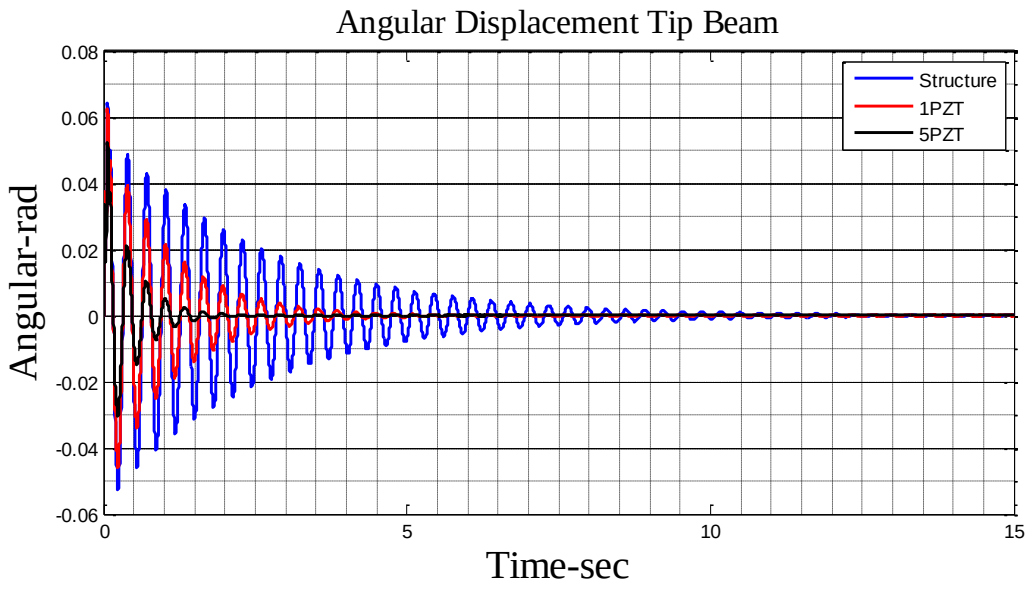

Figure 22 Impulse Angular Displacement

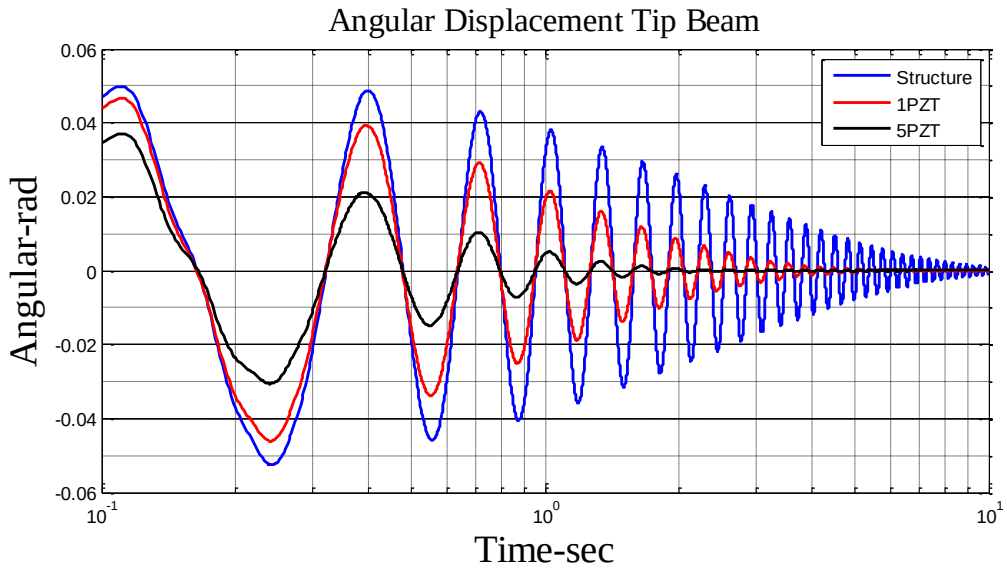

Figure 23 First Seconds Impulse Angular Displacement

Table 5 Optimal Values of Impulse Input

		1 PZT	
Objectives	Min.Time(sec)	1.7347	1.6092
	Max.Disp (m)	1.1495×10^{-6}	$\mathbf{2.7554 \times 10^{-5}}$
Element Location		12	[48,89,56,25,27]
LQR	α_1	37.303	56.774
	α_2	86.431	79.522
	γ	0.806	0.028

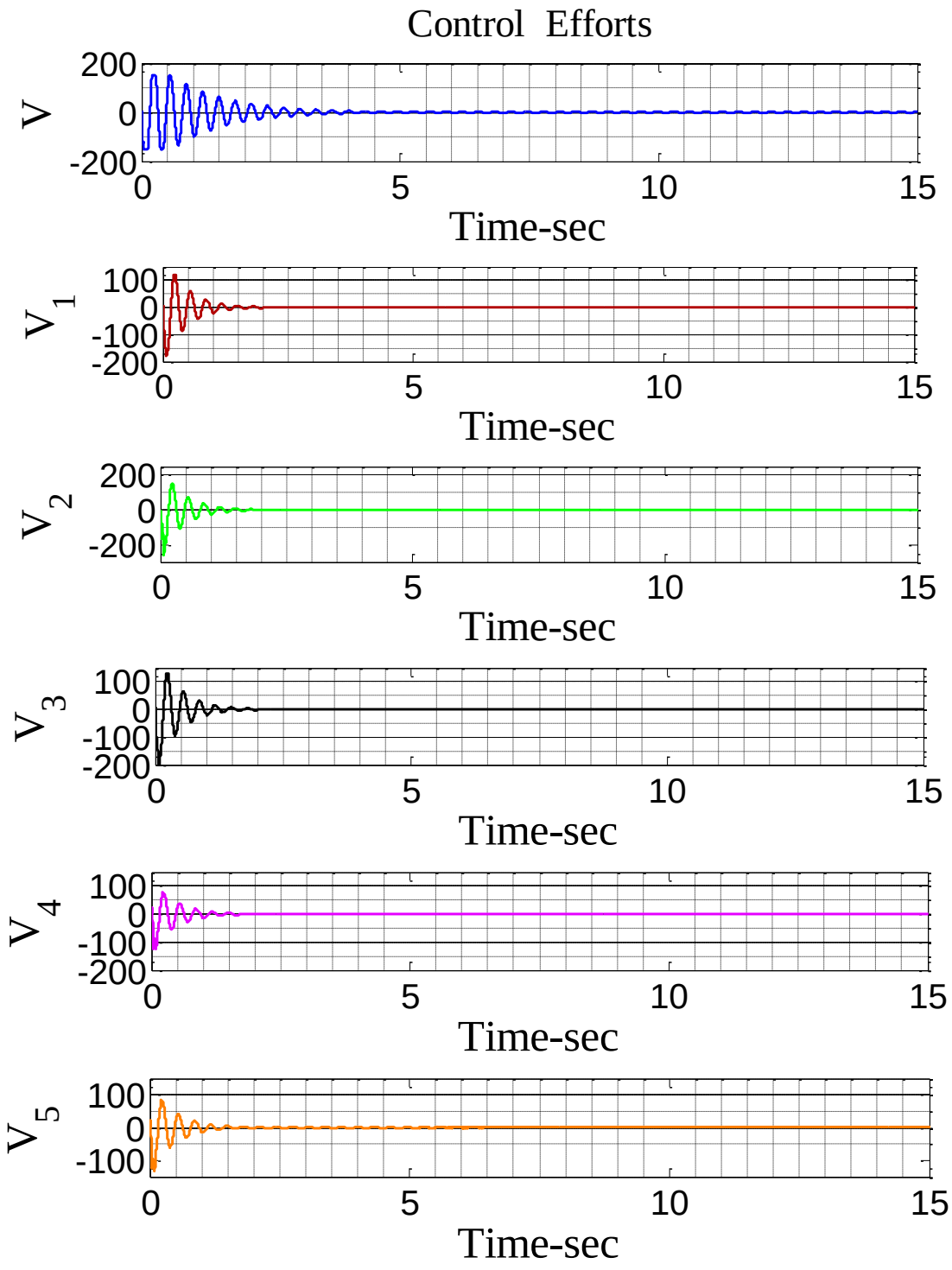

Figure 24 Impulse Voltage Actuators for 1PZT-5PZT Models

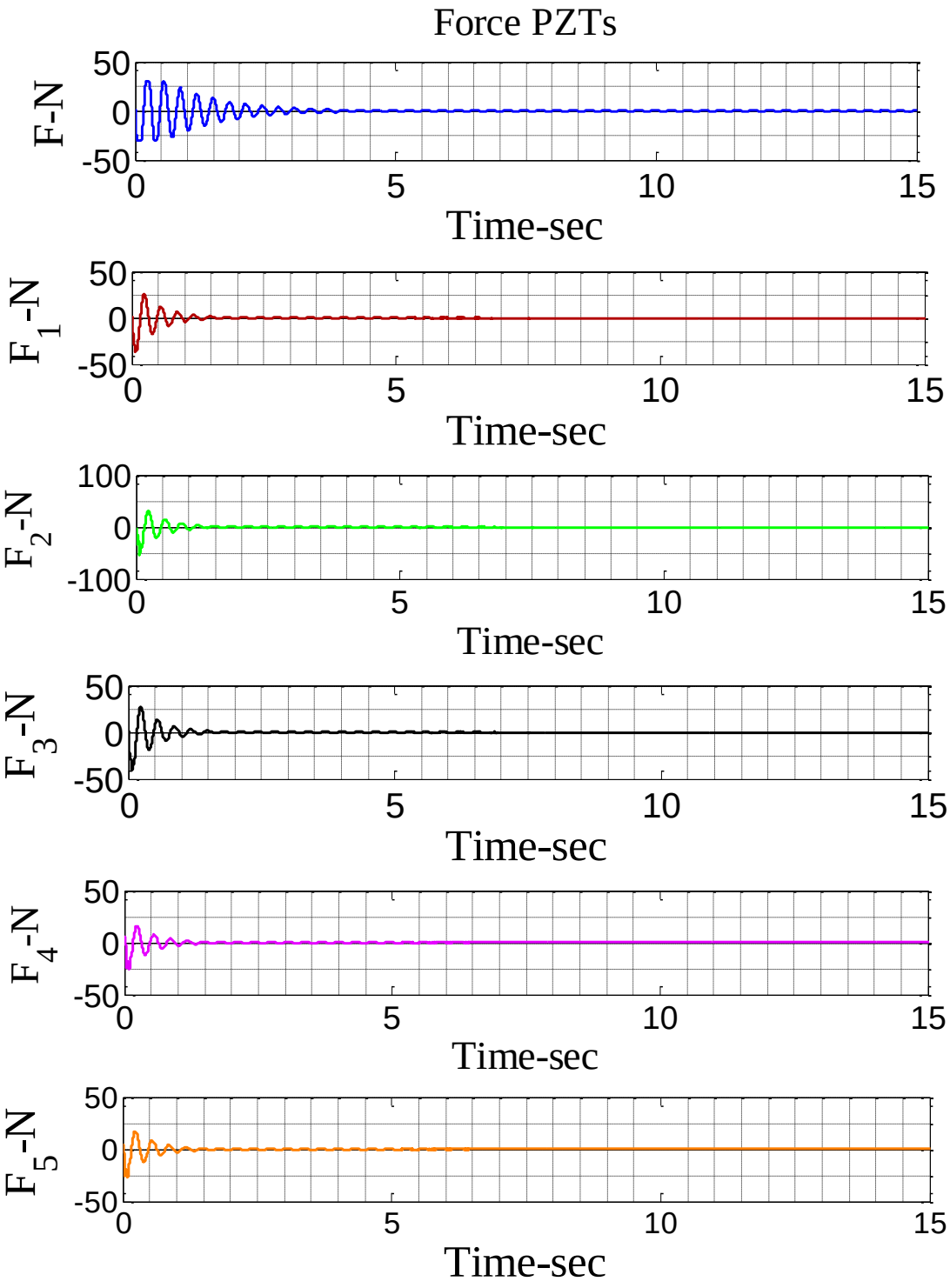

Figure 25 Impulse Force Actuators for 1PZT-5PZT Models

6 Conclusions

This study attempted to automatically control a cantilever beam model from external stimulations by piezoelectric and conduct vibration attenuation in system. Using finite element method, system equations were designed in MATLAB Software. Then, by embedding LQR-MOPSO controller attenuated the system.

Here, it has been attempted to stimulate the system with Step and Impulse inputs so that LQR-MOPSO controller design verification would be reliable. According to the results in the figures and tables (4) and (5), the followings are concluded:

1) Validation of the modeling and locating approach due to the coordination of input and output.
2) Identifying critical points due to increased piezoelectric element.
3) Minimized vibration attenuation time in 5PST than 1PZT due to lower energy waste.
4) Minimized transient response of 5PST than 1PZT due to physical difference of the model.
5) Different signs of piezoelectric voltage with displacement of the beam tip.
6) Increasing the number of piezoelectric patches has a significant effect on detecting critical points.
7) 5PZT model has a more optimal attenuation compared to 1PZT.
8) More vibration modes can be controlled with 5PZT rather than 1PZT.
9) Minimum vibration attenuation time compared to 1PZT due to lower power loss
10) According to reference [14], the voltage of actuators in 5PZT and voltage of actuators in 1PZT are logical and feasible values.
11) According to locating piezoelectric patches on the beam, stiffness and mass change and this leads to beam displacement. This can be observed in all graph with logarithmic horizontal axis.
12) Despite designing an LQR controller for 5 pairs of piezoelectric sensor and actuator element in 5PZT, MOPSO determined controller coefficients so that 5 pairs of piezoelectric sensor are covered for vibration attenuation of the beam structure and present a significant attenuation compared with 1PZT.
13) Negative voltage in piezoelectric actuator input indicates positive displacement of the tip of the beam (upward displacement) and positive voltage in actuators indicates negative displacement of the tip of the beam (downward displacement).
14) By observing figures related to piezoelectric actuator voltage (optimized tables extracted from optimizing operation) in Step and Impulse inputs it can be understood that locations determined by MOPSO algorithm is in the beginning of the beam and close to backrest and fewer voltages are deployed compared to elements that are far from the backrest. When the transverse load force is closer to the backrest, less displacement would happen.
15) If location coordinates of the elements determined by MOPSO in 1PZT is mapped to location coordinates in 5PZT, it can be seen that location coordinates are different in 1PZT and 5PZT. The main reason of the difference is the beam physics due to dividing one pair of piezoelectric element into 5 pairs of smaller elements and locating them along the beam, which leads to change in beam stiffness and mass, and finally change in dynamic behavior of the beam.

Reference

[1] Quek, S.T., Wang, S.Y., and Ang, K.K., “Vibration Control of Composite Plates via Optimal Placement of Piezoelectric Patches”, Journal of Intelligent Material Systems and Structures. Vol. 14, Issue. 4-5, pp. 229-245, (2003).

[2] Liu, W., Hou, Z., and Demtriou, M.A., “A Computational Scheme for the Optimal Sensor/Actuator Placement of Flexible Structures using Spatial H_2 Measures”, Mechanical System and Signal Processing, Vol. 20, pp. 881-895, (2006).

[3] Gua, H.Y., Zhang, L., Zhang, L.L., and Zhou, J.X., "Optimal Placement of Sensors for Structural Health Monitoring using Improved Genetic Algorithms, Smart Material and Structures", Vol. 13, No. 528, pp. 528-534, (2004).

[4] Da Rocha, T.L., Da Silva, S., and Lopes Jr, V., "Optimal Location of Piezoelectric Sensor and Actuator for Flexible Structures", 11th International Congress on Sound and Vibration, 5-8, St. Petersburg, Russia, pp. 5-8, (2004).

[5] Dos.Santoes, E., Lucato, S.L., Mc Meeking, R.M., and Evans, A.G., "Actuator Placement Optimization in A Kagome Based High Authority Shape Morphing Structure", Smart Materials and Structures, Vol. 14, No. 86, pp. 875, (2005).

[6] Brasseur, M., Boe, P.D., Gdinval, J.C., Tamaz, P., Caule, P., Embrechts, J.J., and Nemerlin, J., "Placement of Piezoelectric Laminate Actuator for Active Structural Acoustic Control", International ISMA, KU Leuven, Belgium, pp. 1-14, (2004).

[7] Ning, H.H., "Optimal Number and Placements of Piezoelectric Patch Actuators in Structural Active Vibration Control", Engineering Computations, Vol. 21, No. 6, pp. 601-665, (2004).

[8] De Oliveira, A.S., and Junior, J.J.L., "Placement Optimization of Piezoelectric Actuators in a Simply Supported Beam through SVD Analysis and Shape Function Critic Point", 6th World Congress of Structural and Multidisciplinary Optimization, Rio de Juneiro, Brazil, (2005).

[9] Wang, S.Y., Tai, K., and Quek, S.T., "Topology Optimization of Piezoelectric Sensors/Actuators for Torsional Vibration Control of Composite Plates, Smart Materials and Structures", Vol. 15, pp. 253-269, (2006).

[10] Lottin, J., Formosa, F., Virtosu, M., and Brunetti, L., "About Optimal Location of Sensors and Actuators for the Control of Flexible Structures", 7th International Workshop on Research and Education in Mechatronics, KTH University, Stockholm, Sweden, pp. 1-5, (2006).

[11] Lottin, J., Formosa, F., Virtosu, M., and Brunetti, L., "Optimization of Piezoelectric Sensor Location for Delamination Detection in Composite Laminates", Engineering Optimization, Vol. 38, No. 5, pp. 511-528, (2006).

[12] Belloli, A., and Ermanni, P., "Optimum Placement of Piezoelectric Ceramic Modules for Vibration Suppression of Highly Constrained Structures", Smart Materials and Structures, Vol. 16, pp. 1662-1671, (2007).

[13] Qiu, Z.C., Zhang, X.M., Wu, H.X., and Zhang, H.H., "Optimal Placement and Active Vibration Control for Piezoelectric Smart Flexible Cantilever Plate", Journal of Sound and Vibration, Vol. 301, pp. 521-543, (2007).

[14] Roy, T., and Chakraborty, D., "GA-LQR Based Optimal Vibration Control of Smart FRP Composite Structures with Bonded PZT Patches", Journal of Reinforced Plastics and Composites, Vol. 28, pp. 1383, (2009).

[15] Safizadeh, M.R., Mat Darus, I.Z., and Mailah, M., "Optimal Placement of Piezoelectric Actuator for Active Vibration Control of Flexible Plate", Faculty of Mechanical Engineering Universiti Technologi Malaysia (UTM) 81310 Skudai, Johor, Malaysia.

[16] Yang, J.Y., and Chen, G.P., "Actuator Placement and Configuration Direct Optimization in Plate Structure Vibration Control System", International Conference on Measuring Technology and Mechatronics Automation, Beijing, China, Vol. 1, pp. 407-411, (2011).

[17] Yang, J., and Chen, G., "Optimal Placement and Configuration Direction of Actuators in Plate Structure Vibration Control System", 2nd International Asia Conference on Informatics in Control, Automation and Robotics, Wuhan, China, DOI: 10.1109/CAR.2010.5456890, (2010).

[18] Gupta, V., Sharma, M., and Thakur, N., "Optimization Criteria for Optimal Placement of Piezoelectric Sensors and Actuators on a Smart Structure: A Technical Review", Journal of Intelligent Material Systems and Structures, Vol. 21, Issue. 12, pp. 1-17, (2010).

[19] Trajkov, M., and Nestorvic, T., "Optimal Placement of Piezoelectric Actuators and Sensors for Smart Structures", 15th International Conference on Experimental Mechanics, Porto/Portugal, pp. 1-13, (2012).

[20] Bachmann, F., Bergamini, A.E., and Ermanni, P., "Optimum Piezoelectric Patch Positioning: A Strain Energy-Based Finite Element Approach", Journal of Intelligent Material Systems and Structures, Vol. 23, pp. 1575-1591, (2012).

[21] Zhang, J., He, L., and Wang, E., "Active Vibration Control of Piezoelectric Intelligent Structures", Journal of Computers, Vol. 5, No. 3, pp. 401-409, (2010).

[22] Molter, A., Fonseca, J.S.O., and Bottega, V., "Simultaneous Piezoelectric Actuator and Sensors Placement Optimization and Optimal Control Design for Flexible Non-prismatic Beams, 20th International Congress of Mechanical Engineering", November 15-20, Gramado, RS.Brazil, (2009).

[23] Nowak, L., and Zielinski, T.G., "Determining the Optimal Locations of Piezoelectric Transducers for Vibroacoustic Control of Structures with General Boundary Conditions", Institute of Fundamental Technological Research, Polish Academy of Sciences ul.Pawinskiego 5B, 02-106 Warsaw, Poland.

[24] Rosi, G., Paccapeli, R., Ollivier, F., and Pouget, J., "Optimization of Piezoelectric Patches Positioning for Passive Sound Vibration Control of Plates", Journal of Vibration and Control, Vol. 19, Issue. 5, pp. 1-16, (2012).

[25] Daraji, A.H., and Hale, J.M., "The Effect of Symmetry on Optimal Transducer Location for Active Vibration Control", Proceedings of the ASME 2012 International Design Engineering Technical Conference & Computers and Information in Engineering Conference IDETC/CIE, Chicago. IL, USA, (2012).

[26] Hale, J.M., and Daraji, A.H., "Optimal Placement of Sensors and Actuators for Active Vibration Reduction of a Flexible Structure using a Genetic Algorithm Based on Modified H_∞", Modern Practice in Stress and Vibration Analysis, Journal of Physics, Conference Series. 382, pp. 1-7, (2012).

[27] Zoric, N.D., Simonovic, A.M., Mitrovic, Z.S., and Stuper, S.N., "Multi-objective Fuzzy Optimization of Sizing and Location of Piezoelectric Actuators and Sensors", FME Transactions Vol. 40, pp. 1-9, (2012).

[28] Schulz, S.L., Gomes, H.M., and Awruch, A.M., "Optimal Discrete Piezoelectric Patch Allocation on Composite Structures for Vibration Control Based on GA and Modal LQR", Computers and Structures, Vol. 128, pp. 101-115, (2013).

[29] Chhabra, D., Bhushan, G., and Chandra, P., "Optimal Placement of Piezoelectric Actuators on Plate Structures for Active Vibration Control using Modified Control Matrix and Singular Value Decomposition Approach", International Journal of Mechanical, Industrial Science and Engineering, Vol. 7, No. 3, pp. 1-6, (2013).

[30] Botta, F., Dini, D., Schwingshackl, C., Mare, L.D., and Cerri, G., "Optimal Placement of Piezoelectric Plates to Control Multimode Vibrations of a Beam", Advances in Acoustics and Vibration, Vol. 2013, Article ID905160, pp. 1-8, (2013).

[31] Araujo, A.L., Madeira, J.F.A., Soares, C.M.M., and Soares, C.A.M., "Optimal Design for Active Damping in Sandwich Structures using the Direct Multi Search Method", Composite Structures Vol. 105, pp. 29-34, (2013).

[32] Wrona, S., and Pawelczyk, M., "Controllability Oriented Placement of Actuators for Active Noise Vibration Control of Rectangular Plate using A Memetic Algorithm", The Journal of Institute of Fundamental Technological of Polish Academy of Science, Vol. 38, No. 4, pp. 529-526, (2013).

[33] Worna, S., and Pawelczyk, M., "Application of a Memetic Algorithm to Placement of Sensors for Active Noise-vibration Control", Mechanics and Control, Vol. 32, No.3, (2013).

[34] Takezam, A., Makihara, K., Kogiso, N., and Kitramura, M., "Layout Optimization Methodology of Piezoelectric Transducers in Energy-recycling Semi-active Vibration Control Systems", Journal of Sound and Vibration, Vol. 333, pp. 327-344, (2014).

[35] Dafang, W., Liang, H., Bing, P., Yuewu, W., and Shuang, W., "Experimental Study and Numerical Simulation of Active Vibration Control of a Highly Flexible Beam using Piezoelectric Intelligent Material", Aerospace Science and Technology, Vol. 37, pp. 10-19, (2014).

[36] Li, F.M., and Lv, X.X., "Active Vibration Control of Lattice Sandwich Beams using the Piezoelectric Actuator/Sensor Pairs", Composite Part B: Engineering, Vol. 67, pp. 571-578, S1359-8368-00327-8, DOI: http://dx.doi.org/10.1016/j.compositesb.2014.08.016 , (2014).

[37] Kwak, M.K., and Yang, D.H., "Dynamic Modelling and Active Vibration Control of a Submerged Rectangular Plate Equipped with Piezoelectric Sensor and Actuator", Journal of Fluids and Structures, Vol. 54, pp. 848-867, (2015).

[38] Khorshidi, K., Rezaei, E., Ghadimi, A.A., and Pagoli, M., "Active Vibration Control of Circular Plate Coupled with Piezoelectric Layers Excited by Plane Sound Wave", Applied Mathematical Modelling, Vol. 39, Issues. 3-4, pp. 1217-1228, (2015).

[39] Trindade, M.A., Pagani, Jr, C.C., and Oliveira, L.P.R., "Semi-model Active Vibration Control of Plates using Discrete Piezoelectric Model Filter, Journal Sound and Vibration", Vol. 351, pp. 17-28, (2015).

[40] Zhang, S.Q., Li, Y.X., and Schmidt, R., "Active Shape and Vibration Control for Piezoelectric Bonded Composite Structures using Various Geometric Nonlinearities", Composite Structures, Vol. 122, pp. 239-249, (2015).

[41] Yildirim, K., and Kucuk, I., "Active Piezoelectric Vibration Control for a Timoshenko Beam", Journal of the Franklin Institude, Vol. 353, pp. 95-107, (2016).

[42] Selim, B.A., Zhang, L.W., and Liew, K.M., "Active Vibration Control of FGM Plates with Piezoelectric Layers Based on Reddy's Higher Order Shear Deformation Theory", Composite Structures, Vol. 155, pp. 118-134, (2016).

[43] Abedlijaber, O., Avci, O., and Inman, D.J., "Active Vibration Control of Flexible Cantilever Plate using Piezoelectric Materials and Artificial Neural Network", Journal of Sound and Vibration, Vol. 363, pp. 33-53, (2015).

[44] Plattenburg, J., Dreyer, J.T., and Singh, R., "Vibration Control of a Cylindrical Shell with Concurrent Active Piezoelectric Patches and Passive Cardboard Liner", Mechanical Systems and Signal Processing, Vol. 91, pp. 422-437, (2016).

[45] Selim, B.A., Zhang, L.W., and Liew, K.M., "Active Vibration Control of CNT-reinforced Composite Plates with Piezoelectric Layers Based on Reddy's Higher-order Shear Deformation", Composite Structures, Vol. 163, pp. 350-364, (2017).

[46] Song, Z.G., Zhang, L.W., and Liew, K.M., "Active Vibration Control of CNT-reinforced Composite Cylindrical Shells via Piezoelectric Patches", Composite Structures, Vol. 158, pp. 92-100, (2016).

[47] Manjunath, T.C., and Bandyopadhyay, B., "Vibration Control of Timoshenko Smart Structure using Multirate Output Feedback Based Discrete Sliding Mode Control for SISO Systems", Journal Sound and Vibration, Vol. 326, pp. 50-74, (2009).

[48] Rao, S.S., "*Mechanical Vibrations*", 5th Edition, Prentice Hall Press, New Jersey, ISBN 978-0-13-212819-3, pp. 737, (2011).

[49] Tiersten, H.F., "Linear Piezoelectric Plate Vibrations-elements of the Linear Theory of Piezoelectricity and the Vibration of Piezoelectric Plates", Plenum Press, New York, ISBN : 9781489964533, pp. 1-211, (1969).

[50] Clerc, M., "Particle Swarm Optimization", Wiley Press, Brazil, ISBN-13:978-1-905209-04-0, (2005).

[51] Clerc, M., and Kennedy, J., "The Particle Swarm-Explosion Stability and Convergence in a Multidimensional Complex Space", IEEE Transaction on Evolutionary Computation, Vol. 6, Issue. 1, pp. 58-73, (2002).

Nomenclature

A	Cross-Section
A_s	System Matrix
b	width
B_s	Input Matrix
C_s	Output Matrix
c^E	Mechanical Stiffness
C_1	Individual Learning
C_2	Collaborative Learning
d_{31}	Piezo Strain Constant
D	Charge Density
D_s	Smart Structure Damping Matrix
E_b	Young's Modulus of Beam
E_{ce}	Control Effort Matrix
E_{pzt}	Young's Modulus of Piezo
E^p	Electric Field of Piezo
e	Piezoelectric Strian Constant
f	Force Local
F	Force Global
f_t	Total Force
f_e	External Force
f_c	Piezoelectric Force
G	Shearing Modulus
G_c	Electrical Resistance Constant
h	Piezo-Patch Location Vector
I	Inertia Moment
[I]	Identity Matrix
J	Performance Index
K_{be}	Beam Element Stiffness Matrix
K_{smart}	Smart Structure Stiffness Matrix
K_c	Controller Gain
K_s	Stiffness Structure Matrix
K_w	Transverse Stiffness Matrix
K_θ	Angular Stiffness Matrix
K	Shearing Coefficient
K_{SE}	Smart Element Stiffness Matrix
K_{LQR}	Gain LQR Controller
K_p	Piezo-Patch Stiffness Matrix
l_e	Length Element
l_p	Length Piezo-Patch
M	Local Torque
M_s	Mass Structure Matrix
M_w	Transverse Mass Matrix
M_θ	Angular Mass Matrix
M_{SE}	Smart Element Mass Matrix
M_{be}	Beam Element Mass Matrix
M_p	Piezo-Patch Mass Matrix
M_{pzt}	Piezo-Patch Moment
M_{smart}	Smart Structure Mass Matrix

N_a		Acceleration Shape Function
N_θ		Angular Shape Function
N_w		Transverse Shape Function
P		Sensor Characteristic Vector
P		Symmetric Matrix
q		Local Coordinate
$\dot{q}$		Local Velocity of Node
Q	R	LQR Weighted Matric
r_1	r_2	Random Number
S		Mechanical Strain
t		Time
t_b		Beam Thickness
t_p		Piezo-Patch Thickness
T		Kinetic Energy
u(t)		Control Input
U		Potential Energy
v_i		Velocity of Particles
V_a		Actuator Voltage
υ		Poisson's Ratio
w(t)		External Input
w		Transverse Displacement
w_i		Natural Frequencies
w_I		Inertia Constant of PSO
w(x,t)		Transverse Dynamic Displacemnet
W_v		Virtual Work
x_i		Position of Particle
x_{gbest}		Global Repository
x_{pbest}		Personal Repository
x		Horizontal Coordinate
y_{out}		Output System
z		Transverse Coordinate
θ		Angular Displacement
$\theta(x,t)$		Angular Dynamic Displacement
φ		Shearing Constant
ρ		Density
σ		Mechanical Stress
ε^S		Electric Permittivity
S		Mechanical Strain
α	β	Damping Constants
α_1 α_2	γ	LQR Constants
η		Variables Design
$[\ ]^T$		Transpose Matrix

چکیده

هدف اصلی این تحقیق، کاهش بهینه نوسانات تیر تیموشنکو تحت ورودی‌های غیر متناوب پله و ضربه می-باشد. تیر یکسرگیردار توسط تئوری تیموشنکو و روش عددی اجزاء محدود مدل‌سازی شده و ماتریس‌های سفتی (K)، جرم (M)، دمپینگ (C) استخراج می‌شوند. سپس به منظور مهار ارتعاشات سازه از تکه های پیزوالکتریک بدلیل دارابودن رفتار همزمان ۲ سویه خود، یعنی تبدیل رفتار مکانیکی به رفتار الکتریکی (حسگر) و رفتار الکتریکی به رفتار مکانیکی (عملگر) استفاده شده است.

تکه‌های پیزو الکتریک در دو آرایش متفاوت با ابعاد یکسان و تعداد المان های متفاوت برای ایجاد حلقه کنترلی بکارگرفته شداند. در ادامه با استفاده از کنترلر بهینه درجه دوم (LQR) ارتعاشات سازه میرا شده است. ضرایب وزنی ماتریس های Q و R و مکان تکه های پیزو الکتریک توسط الگوریتم بهینه ساز ازدحام ذرات چند هدفه (MOPSO) مورد جستجو قرار گرفته است. نهایتاً سازه تحت ورودی های استاندارد ضربه و پله قرار گرفته و بر روی نتایج تحلیل و مقایسه صورت می گیرد.